Science of the Total Environment 919 (2024) 170717

Contents lists available at ScienceDirect

Science of the Total Environment

journal homepage: www.elsevier.com/locate/scitotenv

A large flood resets riverine morphology, improves connectivity and enhances habitats of a regulated river

Jhoselyn Milagros Aramburú-Paucar [a], Francisco Martínez-Capel [a,*], Carlos Antonio Puig-Mengual [a], Rafael Muñoz-Mas [a,b], Andrea Bertagnoli [c], Daniele Tonina [c]

[a] Institut d'Investigació per a la Gestió Integrada de Zones Costaneres (IGIC), Universitat Politècnica de València (UPV), 46730 Gandia, Spain
[b] Water Management and Planning Division, Tragsatec, c/ Julián Camarillo 6B, 28037 Madrid, Spain
[c] Center for Ecohydraulics Research, University of Idaho, Boise, ID, USA

HIGHLIGHTS

- Findings support the Intermediate Disturbance Theory (IDT).
- Floods have positive impacts on stream ecological functioning at various scales.
- At the local scale, floods rearrange habitat distribution, enhance habitat diversity, and promote hyporheic exchange.
- At the reach scale, floods increase streambed complexity and hydro-morphological diversity, and improve lateral and vertical connectivity.
- Controlled high flow is an effective strategy to revitalize fluvial forms and riparian habitats.

GRAPHICAL ABSTRACT

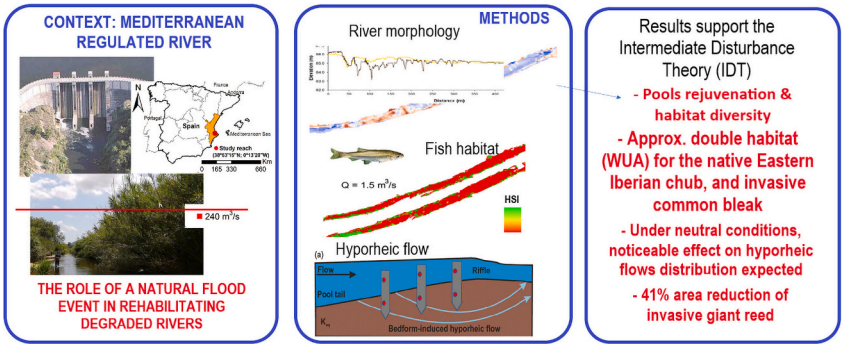

ARTICLE INFO

Editor: Sergi Sabater

Keywords:
Flood flows
Pulse flows
Habitat quality
Hyporheic flow
River restoration
Riparian vegetation, regulated gravel bed river

ABSTRACT

Flow regulation in gravel-bed rivers impacts the hydrology, sediments and morphology, riparian vegetation, and vertical connectivity with the hyporheic zone. In this context, previous works have suggested that flood events may have riverine morphological and ecological benefits. In a Mediterranean-climate river system, we analyzed the impact of a 18-year return period flood on river morphology, riparian vegetation, fish aquatic habitat quality, and hyporheic exchange in a dam-regulated gravel-bed river, Serpis River (Spain). We collected pre- and post-flood riparian vegetation distributions and bathymetries, which were used to develop two-dimensional surface and three-dimensional subsurface numerical models to map surface and hyporheic hydraulics. Results show that the large flood removed the invasive giant reed from large areas, reshaped the in-channel morphology by forming new bars and pools, and enhanced the complexity of the flow field and the hydro-morphological diversity. The habitat availability for the endemic Eastern Iberian chub (*Squalius valentinus*) and invasive bleak (*Alburnus alburnus*) increased. Hyporheic exchange showed limited change under losing conditions, but noticeable under neutral ambient groundwater condition. This study corroborates the beneficial effects that flood events or high flow releases may have on regulated streams and the potential use of high flow pulse as a restoration tool.

* Corresponding author.
E-mail address: fmcapel@upv.edu.es (F. Martínez-Capel).

https://doi.org/10.1016/j.scitotenv.2024.170717
Received 29 August 2023; Received in revised form 17 January 2024; Accepted 3 February 2024
Available online 7 February 2024

1. Introduction

The natural flow and sediment supply regimes form the natural physical template for riverine ecosystems (Poff et al., 1997; Richter et al., 2003). Within the Intermediate Disturbance Theory, IDT, framework, disturbances like wildfires, floods and droughts are key features of natural processes affecting the riverine ecosystems, because they provide a mechanism for ecosystem resetting (Townsend et al., 1997). However, many streams and rivers have regulated flows (Nilsson et al., 2005), which alter the natural flow, thermal, sediment and nutrient regimes (Ward and Stanford, 1995, 1983) potentially modifying not only longitudinal (Vannote et al., 1980) connectivity, but also lateral and vertical connectivity and their temporal occurrence (Amoros et al., 1987; Ward, 1989). Regulated flows also remove many disturbances resulting in an increase in channel stability, lower frequency of competent flows for sediment transport (Church, 1995; Dean and Schmidt, 2013; Grant et al., 2003; Ligon et al., 1995; Schmidt and Wilcock, 2008) and decrease in geomorphic complexity and in river longitudinal and lateral connectivity (Brandt, 2000; Graf, 2006; Williams and Wolman, 1984) due to loss of functional flows (Escobar-Arias and Pasternack, 2010). These hydromorphological alterations may cause changes in riparian vegetation (Benjankar et al., 2016) a decrease in fish abundance and habitat (Bunn and Arthington, 2002; García et al., 2011; Poff and Zimmermann, 2010) and we also suggest reduction in hyporheic flows.

Whereas extreme floods around and larger than 80-year return period events may have detrimental impact on ecosystems (Hajdukiewicz et al., 2018, 2016; Talbot et al., 2018), more common floods less than or around 10-year return period may reset stream-riparian zone morphology (Dean and Schmidt, 2013) and be beneficial to aquatic and riparian ecology (Talbot et al., 2018; Townsend et al., 1997). These high and frequent flows have also been documented to improve the quality of salmon spawning habitat after a flood event that rearranged the morphology of a newly restored reach (Wheaton et al., 2010a). This evidence suggests that large and frequent (above bankfull but not rare) floods could be a useful and efficient tool for riverine restoration (Groll, 2017; Hayes et al., 2018), and therefore align with the environmental flow (e-flow) guidelines adopted in Spain. Those guidelines established high flow releases as one of the fundamental components of e-flows, although majorly unapplied (Mezger et al., 2019). However, their effects on habitat and spatial connectivity have not been systematically documented, especially in Spain, but only in a few experimental releases, like in the Ebro, Pisuerga, and Cardener Rivers (Cortés et al., 2019).

A remarkable flood event, triggered by Storm Gloria, occurred in January 2020 along the Serpis River (Spain). Storm Gloria was a powerful extratropical cyclone that struck the Iberian Peninsula in January 2020, bringing record-breaking rainfall and causing widespread flooding and damage. Storm Gloria caused an intentional release of water from the Beniarrés Dam for safety reasons. The release was notably higher than the highest mean monthly flow of the river. The release along with tributaries' contributions generated near the study site a high discharge with return period for unregulated flows of 18 years.

Here, we documented the impact of this 18-year return period flood on (1) stream morphology, (2) riparian vegetation, (3) hyporheic flows and (4) aquatic habitat distribution. We developed a set of ecohydraulics and hyporheic models for pre- and post-flood topographies in a reach of the regulated section of the Serpis River. We then assessed the changes in stream morphology and riparian vegetation after the flooding event and quantified the effects of those physical changes on rearing habitat quality for three fish species and on hyporheic exchange.

1.1. Study area

The Serpis River Basin encompasses an area of 752 km^2 in the eastern part of Spain (Fig. 1). Originating at an elevation of 1462 m above sea level, the river flows in a southwestern to northeastern direction, covering 74.5 km until it reaches its mouth at the Mediterranean Sea. Despite distinct morphological variations along the river, it has been uniformly classified in the ecotype of mineralized river in the low mountain region, after the guidelines outlined in the European Water Framework Directive (Garófano-Goméz et al., 2011). In the lowest segments of the Serpis River Basin the climate is Mediterranean-Subtropical (after Köppen-Geiger classification).

The Beniarrés Dam is the only large dam regulating the flow in this river (53 m height, and 30 hm^3 of volume), and it is located 40 km upstream from the river mouth. Its primary purpose is providing irrigation flows, which modified the hydrological regime of the Serpis River since its construction in 1958. The dam-regulated flow regime presents an inverted hydrograph, with high monthly flows during the summer, respect to the natural regime regardless of precipitation patterns (Fig. 1). It captures and retains most of sediment inputs from the upstream basin, except during exceptional events when the dam releases high flows. However, tributaries and the steep hillslopes of the limestone gorge provide sediment inputs to the lower Serpis River. The magnitude and frequency of flood events noticeably decrease after dam construction. In the pre-dam period, the highest flood flow was 800 m^3/s recorded in 1922 whereas, after dam construction, the maximum value recorded was 111 m^3/s in January 2017. A gauging site below the dam indicated an average of 1.16 flood events per year in the pre-dam period (flow events above the bankfull level); in contrast, post-dam studies report an average of 0.28 events per year between 1958 and 1998, and 0.42 between 1998 and 2017 (Sanchis-Ibor et al., 2019).

Downstream Beniarrés Dam, the river gradually narrows while traversing the limestone gorge known as "Barranco del Infierno", which ends near town of Villalonga, and then it widens in its lower part. The study site is located where the valley widens, and the floodplain is predominantly occupied by irrigated farmlands, small agricultural holdings, and a considerable proportion of citrus orchards. The average monthly temperature in this area ranges from 11.2 to 26.1 °C, with the highest temperatures typically occurring in August. The riverbanks were completely covered by vegetation consisting of dense monospecific stands dominated by elephant grass (*Arundo donax*) and including blackberry (*Rubus ulmifolius*), along with a few individuals of black poplar (*Populus nigra*) (Fig. 2). The riverbed substrate primarily comprises alluvial sediments consisting of a dominant proportion of medium to large gravel (8–64 mm; with 22 % of area coverage before the flood event), followed by cobbles (64–256 mm) and fine gravel (2–8 mm), and small proportions of boulders (> 256 mm), bedrock, and sand.

The selected 523-m long river reach is located approximately 20.43 km below the Beniarrés dam (distance on river stem) in the municipality of Villalonga (Valencia; Fig. 1). It consists of a sequence of pool and riffle habitat units with no anthropogenic modifications in the main river channel (neither channelisation nor straightening). A small ford is located downstream the study reach (approximately 30 m below the downstream end) and it was avoided in the hydraulic and habitat model. However, the upstream effect of gradient change due to the ford has never been studied since the construction in around 1903. Based on recent observations on site, a small change in the gradient and sediment proportions can be observed only within 7–10 m upstream of the ford. The pre-event mean gradient along the thalweg in the study site was 0.0030, resulting in 0.0036 after the large flood. In addition, on the floodplain (left side) there is a single-lane road (no dikes), which was completely flooded during the Storm Gloria. No relevant signs of channel incision were observed at the reach. This suggests that the potential sediment deficit due to the Beniarrés dam is mitigated in the study site by hillslope processes. Between Beniarrés dam and the study site there are several unregulated torrential tributaries, e.g., Barranc de la Encantada, with a watershed area of 27.4 km^2 and relevant peak flows. These tributaries and the steep slopes of the mountains in the 7-km long gorge section with diverse taluses provide the Serpis river with an important amount of medium-size sediment. Most of the

watershed area between the dam and the study site is classified as presenting moderate (15–40 t/ha year) or high erosion rates (40–100 t/ha year), with small locations showing highest values, according to the studies characterising the erosion risk in the Serpis River Basin (Confederación Hidrográfica del Júcar, 2008).

We conducted this study before and after the Mediterranean Storm Gloria (January 2020) that caused intense precipitations and the consequent intentional release of a flood flow for dam safety. The mean daily flow of 240 m^3/s from the dam release and Serpis tributaries was recorded at the Azud de Carrós gauging station (21st of January 2020) nearly 7 km downstream the study site with no major tributaries between the study site and the gauging station. The governmental Júcar River Basin Authority recorded hourly discharges exceeding 300 m^3/s between 8:00 PM on January 20th and 10:00 AM on February 21st, with a peak hourly discharge of 325 m^3/s, that has an estimated return period of 18 years (Confederación Hidrográfica del Júcar, 2019). This return period is based on historic records of the instantaneous (hourly) unregulated flows as defined by Spanish and European regulations.

2. Methods

In the river section downstream from the limestone gorge, we assessed the habitat diversity and estimated a proportion of 60 % length of pools and 40 % of riffles. According to these proportions, we selected a representative river reach (523 m river length) to perform the topographic survey, hydraulic modelling, and the physical habitat simulation, according to the standard protocols of the Instream Flow Incremental Methodology, IFIM (Bovee et al., 1998). There we applied different techniques as we further explain below; i) we surveyed pre- and post-flood riverine topographies and riparian vegetation; ii) hyporheic exchange was measured at ten locations to validate a three-dimensional hyporheic model and to quantify hyporheic fluxes for both pre- and post-flood scenarios; iii) two-dimensional hydraulic models were developed with pre- and post-flood topographies, then habitat evaluation was compared for three fish species. The predicted flow hydraulics supported a fuzzy-logic suitability-index-based (SI-based) ecohydraulic model (Bovee, 1978; Noack et al., 2013) that simulated rearing habitat quality distribution for three fish species and a three-dimensional hyporheic model. Aerial photography allowed us to map changes in riparian vegetation for pre- and post-flood conditions.

Performance between predicted and measured quantities was evaluated by quantifying the mean ME, and standard deviation, SD, of the residuals, R, between measured, O, and simulated, S, quantities, e.g., water surface elevation, depth averaged velocity, streambed elevation changes and hyporheic flux:

$$ME = \frac{1}{NC}\sum_{i=1}^{NC} O_i - S_i = \sum_{i=1}^{NC} \frac{R_i}{NC} \quad (1)$$

$$SD = \sqrt{\frac{\sum_{i=1}^{NC}(R_i - ME)^2}{NC - 1}} \quad (2)$$

where NC is the total number of measurements.

2.1. Morphologic characterization

2.1.1. Pre & post flooding river channel survey

The remote sensing data was acquired utilizing a Phantom 4 Pro drone, equipped with a 20-Megapixel camera and a 1-in. sensor (average flight altitude of 50 m). The purpose was to obtain highly detailed aerial images with a high resolution (approximately 1–2 cm). DJI GS Pro© software was employed to pre-program the flight path and configure parameters for all surveys. Before conducting the flights, Ground Control Points (GCPs) and Check Points (CPs) were established in the field using coded targets. Approximately 66 % of these points were designated as GCPs to facilitate georeferencing, while the remaining 34 % served as CPs to validate the accuracy of the very-high-resolution digital terrain model (Conesa-García et al., 2022, 2020; Puig-Mengual et al., 2021). The topographic survey of the coded markers was conducted using a GPS-RTK Prexiso G5©. This GPS was also used to collect all the submerged data we used to construct the digital terrain model (DTM) of the complete river channel and banks. To ensure accurate identification of corresponding points, consistent overlaps of 80 to 90 % between consecutive images were maintained (Seifert et al., 2019).

The acquired data were processed using Agisoft PhotoScan Pro v.1.2.2© software. This software employed the structure-from-motion photogrammetry technique to generate point clouds, continuous textured meshes, and VHR DTMs for each survey event (pixel size 0.02 m), as well as orthomosaics (Conesa-García et al., 2022, 2020; Puig-Mengual et al., 2021). These final products were georeferenced in the WGS84 system for subsequent analysis. The same remote sensing

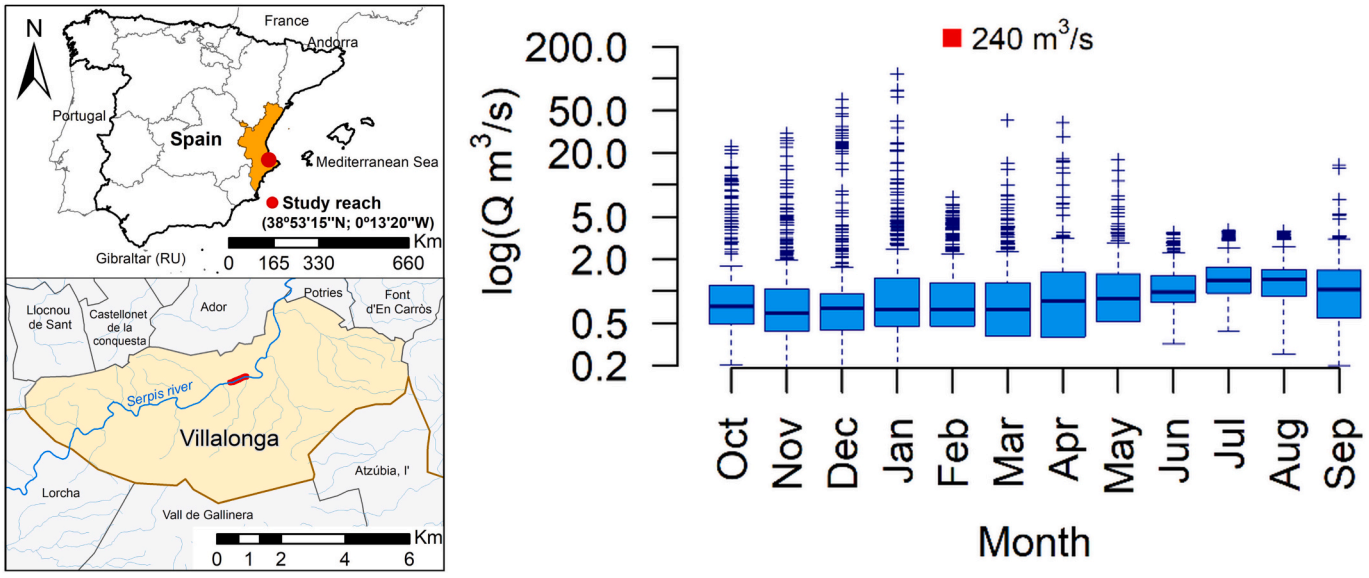

Fig. 1. Study site location within Spain, Europe (left, top) and along the Serpis River (left bottom) and flow regime (monthly scale) (right) in the form of box and whiskers (crosses indicate outliers), from October 1998 to September 2017 (regulated flow data). The red square indicates the magnitude of this study flood-flow event (mean daily flow, 21st January 2020).

procedure and the survey in the submerged part of the river channel were equally performed before and after the Storm Gloria (i.e., pre-flood and post-flood scenario). The DTM depicting the topography for the hydraulic model in the simulation river reach and the DTM of differences was used to detect changes (Wheaton et al., 2010b).

To evaluate the morphological changes and assess the event-scale sediment budget along the river reach, the two digital elevation models of the riverbed (before versus post-flood) were used to calculate a set of statistical parameters (Conesa-García et al., 2020, 2022). Specifically, the values of the total area of interest (m2), total volume

Fig. 2. Different views of the Serpis River in the study segment in pre-flood (upper panel) and post-flood (middle and lower panel) conditions. Upper left: Boulders in the lower part and right bank (background) colonized by *Arundo donax* in pre-flood condition (looking downstream). Upper right: general view from the river channel where complete coverage of *Arundo donax* was observed on the right bank in pre-flood condition (looking downstream). Middle left: side arm of the river after erosion and cane uprooting; pieces of canes and rhizome can be observed (post-flood). Middle right: Left bank and large gravel bar created after the flood, where some of the sensors were located. Lower left: new habitat with cobbles and boulders deposited on the left bank and new rapid created just upstream of the simulated river reach (observe one person standing on the left bank). Lower right: most of the soil and sediment was eroded in the right toe of the bank; part of the rhizome and cane remained.

difference average (m3), net thickness difference (m), and percent imbalance (departure from equilibrium), among other variables, were estimated in ArcGis 10.5 © (ESRI, Redlands, CA, USA), by subtracting the final topography from the previous topography for the same area (Calle et al., 2018). Consequently, the errors associated with the use of two surface models to determine volumetric sediment budgets were described and assumed for each comparative survey analysis, according to Brasington et al. (2003).

The pre- and post-flood flow hydraulic complexities were quantitatively assessed by comparing the pre and post Hydro-Morphological Index of Diversity (HMID) index proposed by Gostner et al. (2013). The HMID was specifically designed to assess reach-scale heterogeneity for engineering programs involving geomorphic measures, as well as long-term streambed evolution at a catchment scale. HMID serves as a metric to evaluate flow heterogeneity based on flow depth and depth-averaged velocity. It incorporates their partial diversity, *Pd*, metric defined as:

$$Pd_i = 1 + \frac{\sigma_i}{\mu_i} \tag{3}$$

where μ is the mean and σ standard deviation, quantified at the reach scale, of *i*-th variable here the depth-averaged velocity (v) and local depth (d). Notice that $\frac{\sigma_i}{\mu_i}$ is the coefficient of variation of *i*-th variable. The HMID is defined as the sum of the squares of the partial diversity coefficients:

$$HMID = \left(1 + \frac{\sigma_v}{\mu_v}\right)^2 \bullet \left(1 + \frac{\sigma_d}{\mu_d}\right)^2 \tag{4}$$

Previous approaches made comparisons based on means and coefficients of variation of water depth, near-bed and depth-averaged flow velocity, and bed material grain size (Hajdukiewicz et al., 2018, 2016). HMID can be considered as an evolution of previous approaches and its value has been linked to ecological indicators (Gostner et al., 2013). It does not solely represent physical diversity, since a strong correlation was observed between this index and Rapid Bioassessment Protocols (Barbour et al., 1999), a visually-based habitat assessment tool (Gostner et al., 2013). The results of the HMID were categorized into three classes based on anthropogenic disturbance: morphologically heavily altered sites with HMID <5; median alteration with limited variability of hydraulic units, 5 < HMID <9, and morphologically pristine sites where gravel-bed streams fully exhibit their spatial dynamics with HMID >9.

To ensure a valid comparison under equal flow conditions, hydraulic data were extracted from the simulation performed at the study site (refer to the section below) for the same discharge of 0.86 m^3/s.

2.1.2. Pre & post flooding extension of giant reed (A. donax) and substrate

Riparian vegetation, native and invasive, may reduce the velocity of water flow and increase the hydraulic roughness of the channel and floodplains, which can cause an increase in water depth and therefore increased flood levels (Baptist et al., 2004; Harezlak et al., 2020b). On the other hand, the high velocity during floods can uproot or damage riparian vegetation due to sediment scoring, thus potentially resulting in temporary or permanent loss of vegetation cover (Calvani et al., 2019; Džubáková et al., 2015), depending on different factors. For instance, the development of adventitious roots and stronger structural roots provide more resistance to uprooting (Garófano-Gómez et al., 2016). In this study, the orthomosaic of the complete modelling reach was used to estimate the area and the reduction of giant reed extension after the flooding (ArcGIS 10.5©). Substrate characterization and cover were characterized during the topographic surveys.

2.2. Hyporheic measurements

We installed ten probes to measure near-surface hyporheic fluxes around the two large bars present in the post-flood reach (DeWeese et al., 2017; Gariglio et al., 2013). Each probe was made with a 30-cm-long 1-in.-diameter PVC pipe that housed two temperature sensors 20-cm apart connected to an Arduino data logger that recorded water temperature every 15 min from February 28th to May 28th, 2020. Each probe was manually inserted into the sediment with the top sensor set at the water-sediment interface. We measured the distance from the rim of the pipe to the streambed sediment at installation and removal of the probes. These measurements were used to quantify the quality of temperature predicted hyporheic flows (DeWeese et al., 2017).

The water temperature time series were analyzed with the model proposed by Luce et al. (2013) to extract both hyporheic fluxes and streambed elevation changes (DeWeese et al., 2017; Tonina et al., 2014). The method compares the phase, φ, and amplitude, A, of the temperature signals of two paired sensors separated by a sediment thickness Δz, and quantified the dimensionless number η:

$$\eta = \frac{-ln\left(\frac{A_s}{A_w}\right)}{\varphi_s - \varphi_w} = \frac{-ln(A_r)}{\Delta\varphi} \tag{5}$$

from which the change in streambed elevation, $e_{streambed} = e_{sensor} + \Delta z$ (where e_{sensor} is the elevation of the bottom sensor), and Darcian flux q are quantified.

$$q = \gamma\sqrt{\omega\bar{\kappa}_e\left(\eta + \frac{1}{\eta}\right)}\ \frac{1-\eta^2}{1+\eta^2} \tag{6}$$

$$\Delta z = \Delta\varphi\sqrt{\frac{\bar{\kappa}_e}{\omega}\left(\eta + \frac{1}{\eta}\right)} \tag{7}$$

The average effective thermal diffusivity, $\bar{\kappa}_e$, expresses the thermal property of the sediment and pore-water matrix between the paired sensors and, once it is quantified, is considered a constant in time. It is quantified from the temperature time series obtained during a period, t_p, when Δz is constant and as a known value, Δz_c,

$$\bar{\kappa}_e = \int_{t_p} \kappa_e dt; with\ \kappa_e = \frac{\omega\Delta z_c^2}{\Delta\varphi^2}\frac{\eta}{1+\eta^2} \tag{8}$$

where $\omega = 2\pi/P$ is the expected angular frequency at the analyzed period, P, of the temperature signal which is 1 day in our analysis.

Comparison between measured and predicted streambed elevation at retrieval of the probes (June 1st 2020) shows ME and SD of residual of 5.8 cm and 2.99 cm, which are a little bit higher than those reported in literature (Bray and Dunne, 2017; DeWeese et al., 2017) (see insert table in Fig. 3). The median grain size was about 3 cm, which sets the threshold for detectable streambed elevation changes (DeWeese et al., 2017). Additionally, measuring the elevation around the probes was challenging as there were variations of several centimetres (3–4 cm) around the PVC pipe and algae. Here we use the mean value. Thus, part of this mismatch could be due to field challenges.

2.3. Hydraulic modelling

We used HEC-RAS two-dimensional model to solve the full Saint-Venant equation to simulate surface water. The model requires specifying two parameters: lateral eddy viscosity, which was set at 0.068 m^2/s and a resistance coefficient expressed as a Manning's n. We calibrated and validated the latter by minimizing the residuals between measured and predicted water surface elevation and depth-averaged velocities. We developed a 0.05-m size quadrilateral regular mesh that extended in the nearby floodplain and had the same resolution as the DEM. We imposed discharge at the upstream boundary condition and normal flow at the downstream boundary. We used pre- and post-flood topographies to define the physical domain of the model. The calibrated Manning's n had a value of 0.055 $s/m^{1/3}$ for both pre- and post-flood topographies and minimized the mean, ME, and standard deviation, SD, of the

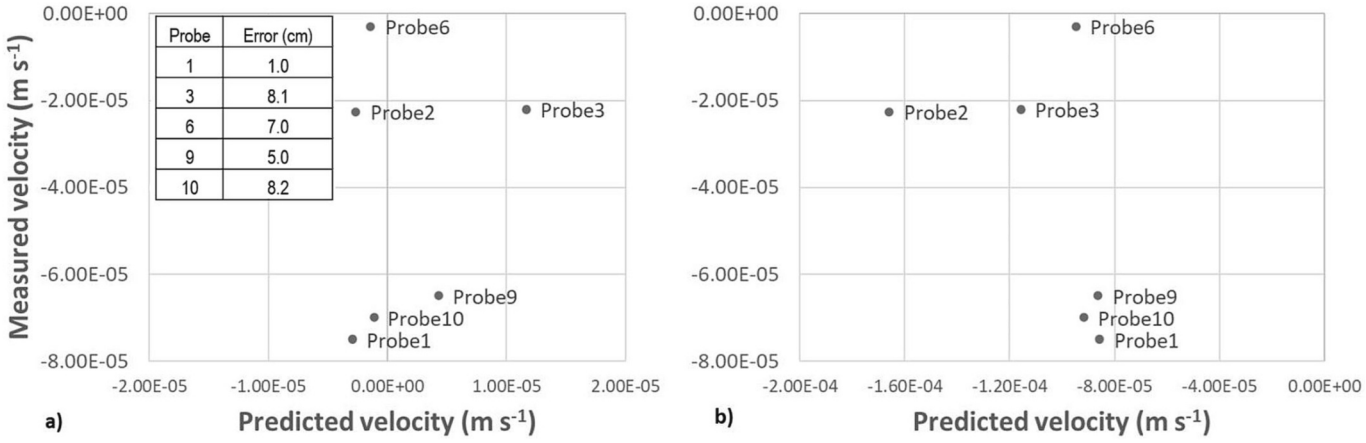

Fig. 3. Comparison between field measured and numerically predicted hyporheic fluxes averaged over the first 0.15 m of sediment for a neutral case (a) and simulating a losing reach (b) with isotropic and homogeneous hydraulic conductivity $K = 0.0193$ cm s^{-1}. The in-figure table provides the residuals of the streambed elevation location measured at the end of the study period and predicted from the thermal analysis.

residuals between measured and predicted water surface elevation, and depth-averaged velocity (Table 1). These values of Manning's *n* could be large since the streambed is gravel but there were several large gravel particles which may have increased local roughness, especially at low flows and were not captured in the topographical survey. The ME and SD values for calibration and validation are in the upper end of those reported in literature for the water surface elevation but within those reported for velocity (Carnie et al., 2015; Kammel et al., 2016; Tonina et al., 2020).

2.4. Habitat suitability assessment

To investigate the effects of the flood event on habitat quality, we developed fuzzy-logic SI-based rearing habitat models supported by the predicted hydraulics for pre- and post-flood scenarios for three fish species. This includes a native species within the Serpis River Basin, the Eastern Iberian chub (*Squalius valentinus*) (Perea and Doadrio, 2015) and two invasive species, the common bleak (*Alburnus alburnus*) and pumpkinseed (*Lepomis gibbosus*), both widely spread over the Iberian Peninsula (Curto et al., 2022; Yavno et al., 2020) and already established in the Serpis River. We used habitat suitability models for depth-average velocity, depth, substrate and cover availability to quantify each cell habitat suitability index, *SI*, within a fuzzy logic approach (Jorde et al., 2001; Mouton et al., 2008; Muñoz-Mas et al., 2012; Noack et al., 2013). The value of SI ranges from 0 (not suitable) to 1 (perfect habitat).

The presence/absence data used to develop the habitat suitability models were retrieved from former studies carried out in the Júcar River Basin District (Muñoz-Mas et al., 2019, 2018a). In these studies, fish presence was surveyed by snorkeling and data on microhabitat conditions: mean flow velocity (m/s), depth (m) substrate composition (%) and cover availability (yes/no), were collected systematically in a regular square grid of 2 m of side length. The percentage of each substrate type was visually estimated within the following classes: silt ($Ø \leq 62$ μm), sand (62 μm $< Ø \leq 2$ mm), fine gravel ($2 < Ø \leq 8$ mm), gravel ($8 < Ø \leq 64$ mm), cobble ($64 < Ø \leq 256$ mm), boulder ($Ø > 256$ mm) and bedrock (Muñoz-Mas et al., 2012) and the observed percentages were summarized into the dimensionless substrate index (Mouton et al., 2011), which ranges between 0 (silt) and 8 (bedrock). The considered types of cover were: caves, reeds, aquatic vegetation, shade, rocks (large cobbles, boulders) and woody debris (Muñoz-Mas et al., 2016).

Zero-order Takagi-Sugeno-Kang FRBSs (Takagi and Sugeno, 1985) were used to develop the habitat suitability models. These models consist of a series of rules such as: IF velocity is Low, Depth is Medium, Substrate is Coarse and Cover is Present THEN the suitability is 1 (i.e., High), describing the suitability related to the different combinations of microhabitat conditions. Fuzzy sets are used to quantify the membership to each category (Zadeh, 1965). Consequently, the transitions between them (e.g., from Low to Medium) are gradual, likewise the suitability is.

Through cross validation and the hill climbing algorithm (Mouton et al., 2008; Muñoz-Mas et al., 2016), we determined the optimal number of categories or fuzzy sets—between two or three—and the cover types that must be present to maximize the habitat suitability (1727 alternative models), whereas the parameters of the membership to each fuzzy set were based on the quantiles (i.e., 25 % and 75 %) of the presence data (Bennetsen et al., 2016; Gobeyn et al., 2017; Muñoz-Mas et al., 2018b).

The habitat quality for the entire reach was quantified with the Weighted Usable Area (WUA) index (Bovee, 1982):

$$WUA = \sum_{i=1}^{NC} SI_i \bullet A_i \quad (9)$$

where *NC* is the number of cells within the wetted area, A_w, of the stream and A_i is the area of the *i*-th cell. This parameter is a function of discharge and provides information on the global quality of the habitat at the reach scale. Rating curves for *WUA* values for rearing life stage of each species were derived for flow rates between 0.2 and 2 m^3/s.

Table 1
Calibration and validation mean (ME) and standard deviation (SD) of the residuals between predicted and measured water surface elevation (WSE) and depth-averaged velocity (Velocity) for Manning's n 0.055 s/m$^{1/3}$.

		Q (m^3/s)	WSE (m)		Velocity (m/s)	
			ME	SD	ME	SD
Pre-flood	Calibration	1.42	−0.013	0.07	−0.061	0.126
	Validation	0.35	0.003	0.095	N/A	N/A
Post-flood	Calibration	9.49	−0.031	0.054	0.093	0.176
	Validation	2.73	−0.02	0.11	−0.009	0.166

2.5. Hyporheic exchange analyses

We developed a three-dimensional hyporheic model with MODFLOW. The model was 530 m long, 60 m wide and 3 m thick. The mesh extended 2 m laterally on the right floodplain, because the stream was confined by bedrock on that side. We use 0.5 m by 0.5 m resolution horizontal cell and fifteen vertical layers whose size progressively increased from 0.1 m at the top to 1 m at the bottom layer. We imposed the predicted water surface elevation within the stream wetted area and extrapolated it laterally to inform the upper boundary conditions. We

imposed the head equal to the upstream and downstream water surface elevations at the upstream and downstream boundaries and impose impermeable layer at the side. We imposed an ambient groundwater basal flux at the bottom layer, which was set to 0 to simulate neutral conditions. Boulders were simulated by imposing 0 hydraulic conductivity on the first layer as their thickness was unknown.

The simulation for testing the performance of the hyporheic model was done with a constant discharge similar to 1.9 m^3/s for which we have predicted water surface elevation and occurred during the monitored period. Measured hyporheic fluxes had all downwelling direction with mean value equal to 0.0054 cm s^{-1} at this stream discharge. Comparison between hyporheic fluxes measured in the field with the temperature probes and predicted by the model helped us constrain the values for a homogenous and isotropic hydraulic conductivity, K = 0.0193 cm s^{-1}. The field measurements from all probe locations always quantified downwelling fluxes also in areas, e.g., downstream riffle, where upwelling was expected (Gariglio et al., 2013; Tonina and Buffington, 2009). At those locations under neutral conditions MODFLOW predicted downwelling conditions (Fig. 3a). This suggested that the reach is in losing condition and we placed a downwelling basal groundwater velocity of 0.00146 cm s^{-1} at 3 m level below the streambed. This basal flow caused a nearly 23 L s^{-1} loss of water from the stream with stream discharge of 1.9 m^3/s. By applying this losing condition, MODFLOW simulations predicted similar hyporheic fluxes to those measured in the field, ME = 0.0063 cm s^{-1} and SD = 0.0074 cm s^{-1}, with predicted values within 96 % of the measured value (Fig. 3b).

3. Results

3.1. Morphology

The pre-flood topography had only one large bar and pool with the rest of the streambed nearly featureless, which resembled a plane-bed river with few large boulders (Montgomery and Buffington, 1998)

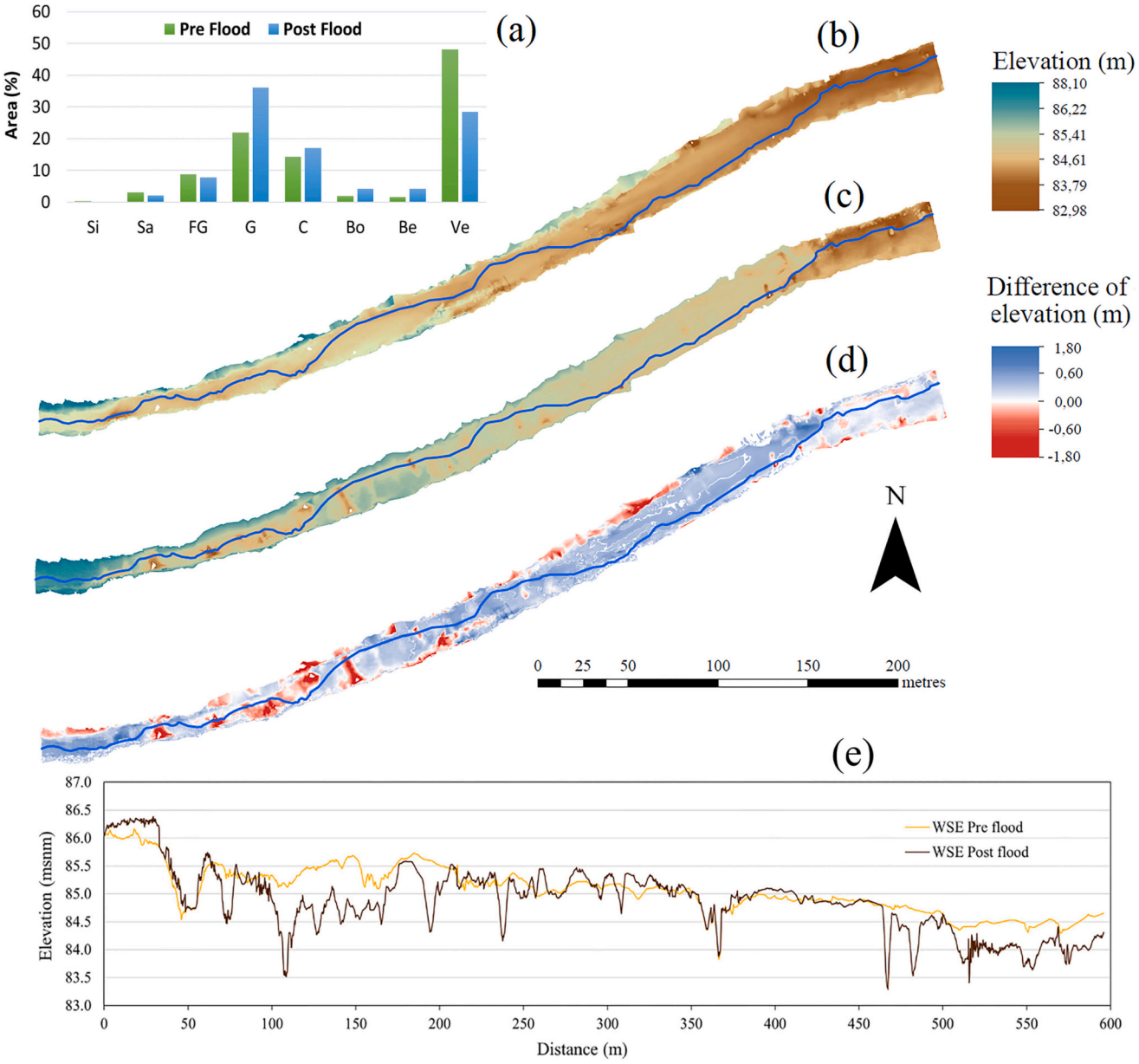

Fig. 4. Column plot for the comparison of substrate types, in percentage of the total area (a), including the riparian vegetation. Digital terrain model (DTM) of the river reaches for pre- (b) and post-flood (c) conditions, their digital elevation difference (d) and streambed elevation changes along their thalwegs (e), which are shown as the solid blue line in b and c.

(Fig. 4a and d). Conversely, the post-flood topography presents more longitudinal and lateral morphological complexity because the flood formed new pools and bars along with extensive scouring around boulders (Fig. 4b–c–d). Sediment transport also changed the sediment patch size and distribution within the streambed and on its banks, where we performed the substrate comparison, including the riparian vegetation (Fig. 4a). Overall grain size distribution presented some relevant changes between pre- and post-flood, and post-flood resulted in looser and less interlocked particles, with lower amount of sand with a 31 % reduction in sand patches. More specifically, the increase of gravel (from 22 to 36 % in area) is related to the removal of sand and finer sediment, the resetting of the side channel on the left side, and the creation of new gravel bars; the same selective transport process applies to the cobbles, which present a smaller increase (see Figs. 2 and 5). In addition, in both banks, the removal of the canes left small proportions of boulders and bedrock exposed (for more detail on the substrate spatial distribution, see Fig. 1 in Supplementary material).

From a quantitative perspective, the sediment budget was estimated based on the two DTMs (Table 2). The average net thickness difference of −0.279 m, the total area of surface lowering in contrast with surface rising (8321 m^2 versus 3207 m^2, respectively), demonstrated that the sedimentary balance was negative, i.e., a clear dominance of erosion over deposition. The general estimation indicated a total net volume difference of 4086 m^3 of sediment; that is, a net degradation in this river reach.

Significant increases in the partial diversity of depth (Pd_d of 1.98 compared to 1.76 pre-flood) and depth-average velocity (Pd_d of 1.86 compared to 1.63 pre-flood) were observed, reflecting increments of 12.5 % and 14.3 %, respectively. HMID value transitioned from a pre-flood medium state 8.21, to a post-flood high level, 13.56. This shift suggests a noticeable achievement in the recovery of natural landforms, with a hydromorphological variability range comparable to that of pristine gravel-bed rivers (HMID>9) (Gostner et al., 2013).

During the flood event, extensive scouring occurred along the banks and floodplain, leading to the exposure of a significant portion of the root system of the invasive giant reed (Fig. 5). Consequently, a substantial area of the riparian zone was cleared of these plants. Conversely, native vegetation, such as oleander (*Nerium oleander*), characterized by deeper root systems and greater stem flexibility, exhibited negligible effects. The removal of giant reed resulted in a reduction of approximately 4244 m^2, representing a decrease of approximately 41 % compared to the initial distribution. This reduction was primarily attributed to the presence of a secondary channel located on the left side of the main channel (north of the main channel in Fig. 5). The existence of this secondary channel facilitated higher flow velocities and contained coarser particles from previous episodes of high discharge, as well as less consolidated particles that were more susceptible to erosion during the flooding event. The roughness, in terms of Manning's *N* for hydraulic modelling was firstly assessed from literature (Arcement and Schneider, 1984; Barnes, 1967). After calibration, it was set at 0.043 in the channel and 0.055 on the banks with dense vegetation stands and large boulders.

Table 2
Statistical descriptors relating to the morphological sediment budgets calculated for the overall river reach under study, for the period between December 2019 (before flood) and February 2020 (after flood). TAI = total area of interest (m^2); TNVD = total net volume difference (m^3); ANTD = average net thickness difference (m) for the area of interest; PI = percent imbalance (departure from equilibrium); TASL = total area of surface lowering (m^2); TASR = total area of surface raising (m^2); UVSL = average unit volume of surface lowering ($m^3\ m^{-2}$); UVSR = average unit volume of surface raising ($m^3\ m^{-2}$); SD = standard deviation of the net thickness differences (m).

TAI	m^2	11,528
TNVD	m^3	4086
	% error	0.027
ANTD	m	−0.279
	% error	−0.026
PI	% value	−0.394
TASL	m^2	8321
TASR	m^2	3207
UVSL	$m^3\ m^{-2}$	0.439
	% error	0.022
UVSR	$m^3\ m^{-2}$	0.135
	% error	0.066
SD	m	0.416

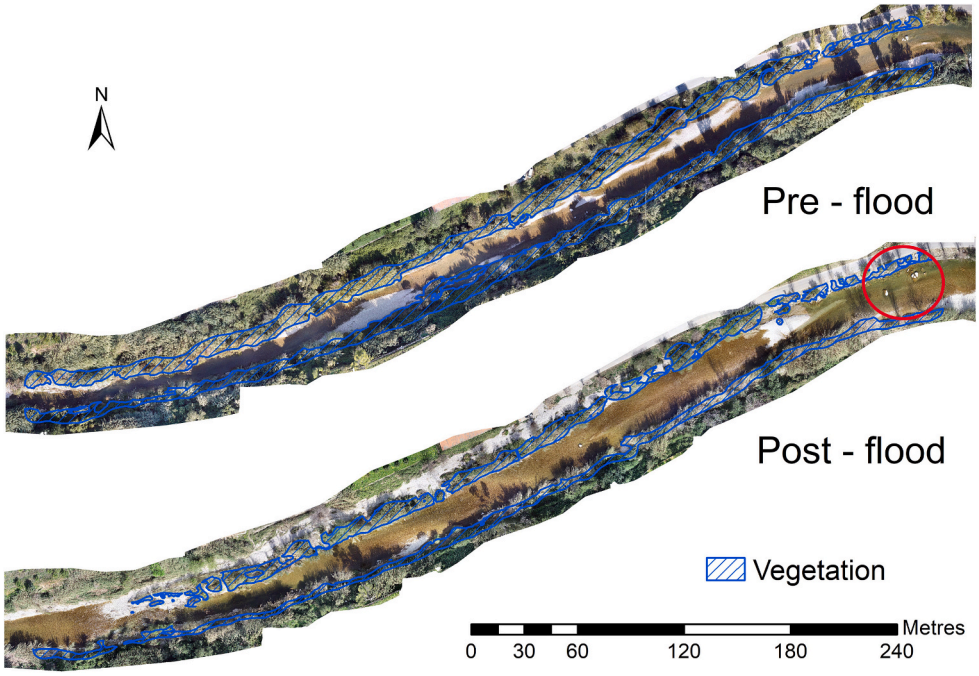

Fig. 5. Mosaic of aerial photograph showing riparian invasive species, giant reed (*Arundo Donax*, in blue polygons), (a) pre-flood distribution with an extent of 10,264 m^2 and (b) post-flood distribution with an extent of 6020 m^2. The red circle indicates location of scour around a few large boulders, which were in pre-flood conditions mostly imbedded in the streambed; ca. 60 m upstream those boulders is the largest and new gravel bar.

3.2. Habitat suitability assessment

The simpler pre- than post-flood streambed morphology displayed less heterogeneity in terms of the hydraulics spatial distribution (Fig. 6). Flow velocity and depth had a very narrow range of variability in the pre-flood condition, which is typical of altered or channelized streams. Conversely, the post-flood topography had a broad range of depth and velocity with pools as deep as 2.6 m and localized fast flows over riffles of nearly 2.7 m/s. The effect of large boulders is visible in the flow field as water moves around or barely submerges them at low flows (red circle in Fig. 6). These features were almost embedded into the streambed in the pre-flood topography. The river length represented in Fig. 6 is shorter than the image in Fig. 5 because some extension near the boundary was removed to avoid boundary effect (in hydraulic terms) for the habitat suitability assessment.

The increase in streambed complexity and, in turn, in the flow field enhanced the aquatic habitat quality for the endemic Eastern Iberian chub and an invasive fish species, the common bleak (Fig. 7). The development or rejuvenation of a pool in the upper part of the river reach (with the first 200 m in length) corresponds to the majority of the highly suitable habitat for the native species, although other micro-habitats by the riverbanks also show some improvements. These changes resemble in a great manner, although in smaller magnitude, the best microhabitats for the common bleak. On the contrary, some of the very suitable microhabitats for the (invasive) pumpkinseed near the banks changed or disappeared after the morphological changes, and we only observed some enhancement in the lowest part of the pool, which did not compensate the habitat loss.

The general results in terms of weighted usable area (WUA) also displayed the aforementioned relevant changes (Fig. 8). Whereas the flood did not change the habitat quality and total extent of the invasive species *L. gibbosus*, the flood did nearly double the habitat in terms of WUA for the native species Easter Iberian chub and common bleak, with ca. 100 % increase in habitat, and even larger magnitude of change in flow conditions below 0.8 m^3/s.

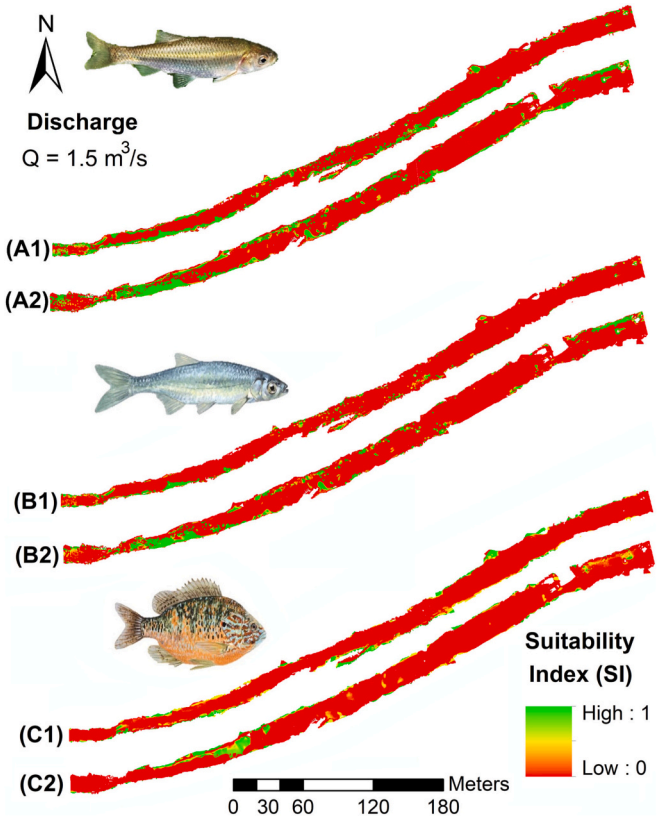

Fig. 7. Pre- (1) and post- (2) flood distribution of habitat quality distribution for the one native species (Eastern Iberian chub, *Squalius valentinus*) (A) and two invasive species (common bleak, *Alburnus alburnus* – B – and pumpkinseed, *Lepomis gibbosus* – C) at the discharge of Q = 1.5 m^3/s.

3.3. Hyporheic exchange

This analysis was based on 5 probes (table in Fig. 3; probes 1, 3, 6, 9 and 10) working the entire study period, whereas the probe 2 stopped recoding after April; other three probes did not work, and one was not found. Point hyporheic measurements showed that the reach recharged the aquifer during the study period (February till June 2020). Assuming the reach would behave similarly in the pre-flood condition, this basal groundwater flow would be strong enough to suppress any hyporheic recirculating cells (Fig. 9a, Table 3). In the post-flood conditions, the scour around few boulders generates local hyporheic recirculating cell (Fig. 9a, b and Table 3) which has limited effect at the reach scale. Under this losing condition, the impact of the flood on hyporheic exchange is

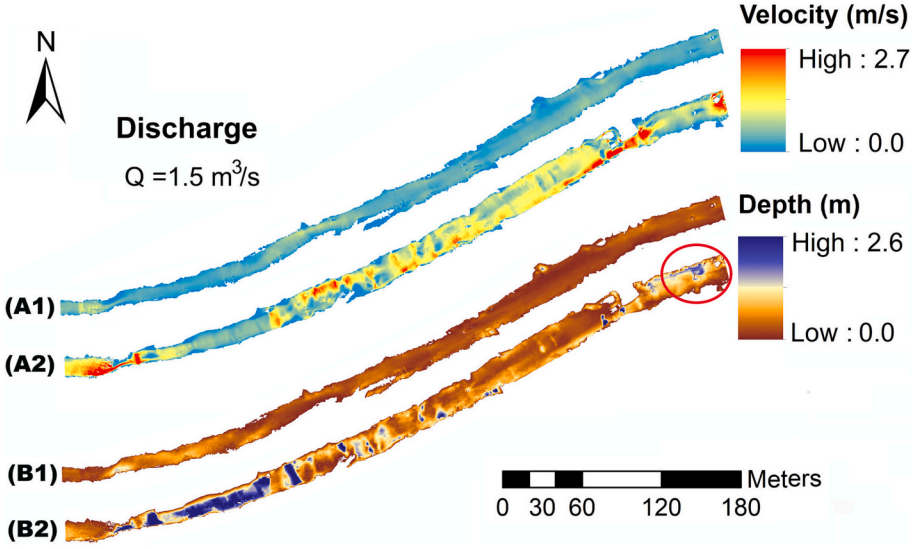

Fig. 6. Velocity (A) and depth (B) distribution at pre (1) and post (2) flood conditions at the same discharge of 1.5 m^3/s. Red circle indicates locations of scour around large boulders, which were in pre-flood conditions mostly imbedded in the streambed. Notice the depth around the boulders.

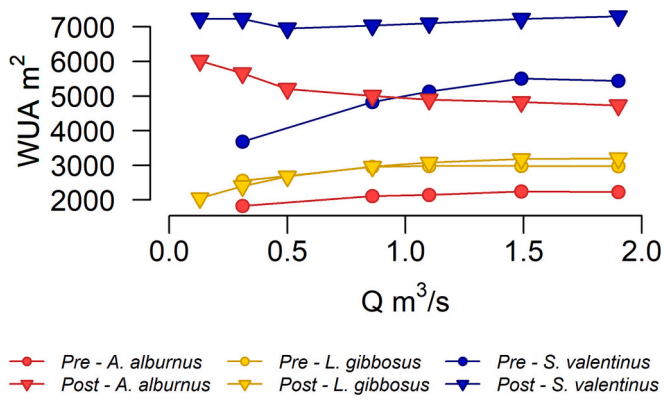

Fig. 8. Weighted usable area (WUA) for the native Eastern Iberian chub (*Squalius valentinus*) and invasive (common bleak *Albumus* and pumpkin seed, *Lepomis gibbosus*) species as a function of discharge for both pre- (full circle marker) and post- (triangle markers) flood periods.

limited as exemplified by nearly identical downwelling flux distributions for pre- and post-flood scenarios (Fig. 10a).

Conversely under neutral conditions, the flood has a noticeable effect on hyporheic flows distribution (Fig. 9c, d) both in terms of fluxes (Fig. 10b) and residence time (Fig. 10c). Hyporheic exchange has faster velocities (Fig. 10b) and shorter hyporheic residence times (Fig. 10c) in the post- than pre-flood conditions. In-stream discharge has a small impact on hyporheic exchange, whose both fluxes and residence times reduce with increasing discharge, which indicates that hyporheic exchange gets shallower with increasing discharge.

4. Discussion

Our results suggest that flood events are important disturbances with the opportunity for ecosystem resetting (Townsend et al., 1997) and fulfilling several ecological functions (Escobar-Arias and Pasternack, 2010). During the annual flood season, large-magnitude peak flows typically transport a significant portion of the annual sediment load and restructure the channel and floodplain landforms, which create the habitat template of the river corridor ecosystem (Yarnell et al., 2015). Such large flows scour the riverbed and the vegetation that encroached on the channel and disperse seeds and wood fragments to rejuvenate riparian vegetation (Petts and Gurnell, 2022). Consequently, peak flows emerge as primary drivers of ecosystem processes that maintain habitat diversity over the long term (Yarnell et al., 2015).

Our analysis focused on short-term effects of the flood on fish habitat quality and hyporheic exchange. The 18-year return period flood induced substantial morphological changes on the banks and the channel. Channels morphological changes include the formation of deeper and more frequent pools, increase in morphological complexity and surface hydraulic heterogeneity (Duffin et al., 2023). These changes were also detected with HMID index, whose value changed between pre- and post-flood, and resulted in the reach to move from medium (HDMI $<$ 9) to pristine (HDMI $=$ 13) status.

This indicates the recovery of natural landforms and ecologically important hydromorphological variability. This increase in ecological status is also supported by the results of the aquatic habitat modelling that showed an increase in the habitat quality for one native and one invasive fish species, although changes were negligible for another invasive species. Therefore, these changes represent an increase in the diversity of habitats and potentially positive effects on the diversity of aquatic species, not only for the two fish species mentioned above but also for others that may be distributed in other sections below the dam. The increase in hydraulic diversity within the study section was accompanied by the creation of a new rapid upstream of the target river stretch, at the location where riparian vegetation had previously established itself on a bar, resulting in the formation of a stable island. The vegetation cover was so dense that detailed topographical surveys were impeded. This section of channel could not be included in the hydraulic and habitat models. Although other studies have documented the dynamics of island development related to woody debris, the new central (small) bar observed in this single channel segment did not show any evidence related to vegetation (Gurnell et al., 2005; Gurnell and Bertoldi, 2020; Mikuś et al., 2013; Revelli et al., 2008; Wohl et al., 2019), as no sign of debris was observed in the gravel or around when the sensors were installed; however, no digging was made in the riverbed to explore this possibility.

An additional change was the creation of pioneer habitats for the riparian vegetation. The flood opened space and allowed pioneer species to recolonize the riparian zone. The invasive giant reed developed such a thick canopy that native species could not grow. The reduction of this invasive plant in terms of percentage was relevant, and this was favoured by the presence of a secondary channel on the left bank, which was covered with vegetation in the pre-flood condition. The presence of the secondary channel was not detected in the pre-flood survey, because the vegetation was very dense and neither walking nor drone survey detected it. However, this secondary channel allowed flood flows to converge and have sufficient shear stress and capacity to uproot vegetation more significantly than expected during the flood. This suggests that a strategy of renewal or rejuvenation of the riparian ecosystem in large areas could notably benefit from some previous local vegetation management; it does not have to reside solely on generating extreme peak flows capable of uprooting rhizomes and stems. On the contrary, it can be significantly facilitated by the maintenance of certain river forms that facilitate the development of localized high shear stresses, even at low flood flows, to balance ecological and economical (preserve sufficient irrigation flows) needs especially in areas where agriculture has an important footprint like this Mediterranean region. This limited riparian vegetation management is potentially necessary in regulated rivers because of constrains on high flows not only for removing invasive species but also to preserve natives (e.g., Benjankar et al., 2020).

Likewise, many river sections in the Júcar River Basin District, the banks of the Serpis River are dominated by large stands of giant reed. These stands develop large stems and rhizomes, which protect them from uprooting. On the other hand, they exhibit a rigid bio-mechanical behaviour (García-Ortuño et al., 2014), which facilitates that the rigid stems and rhizomes can be broken and uprooted during large flooding events. The uprooting and plant transport is an important phenomenon in these rivers because such high-velocity events frequently result in a large mass of woody debris that can collapse structures such as culverts and bridges and poses additional flood risk in the surrounding areas. However, uncertainties in vegetation traits play a key role in ecohydraulic modelling (Lama et al., 2022). Therefore, this information concerning plants removal during flooding is beneficial for river management by supporting decision making on the optimization of floodplain functions (Harezlak et al., 2020a).

The bed scour around boulders has provided new habitats, which were not present before. It allows the formation of hyporheic exchange, which the pre-flood topography did not have because the reach loses water at a rate which overwhelmed any hyporheic flux induced by the pre-flood topography. This localized hyporheic flow has a limited effect at the reach scale. However, the analysis of the reach under neutral conditions shows the beneficial impact of the flood on the hyporheic exchange, which may occur in other reaches along the river and in this site in wetter time periods.

The increase in hyporheic flux under neutral condition is due to the increase in channel morphological complexity, which induced variation of near-bed heads. The post-flood topography has more frequent pools, scours and deposition areas, namely streambed irregularities that induce hyporheic exchange (Gordon et al., 2013), which is not present in the pre-flood topography. Although we could not measure the pre and post flood streambed permeability, post-flood sediment was looser than pre-

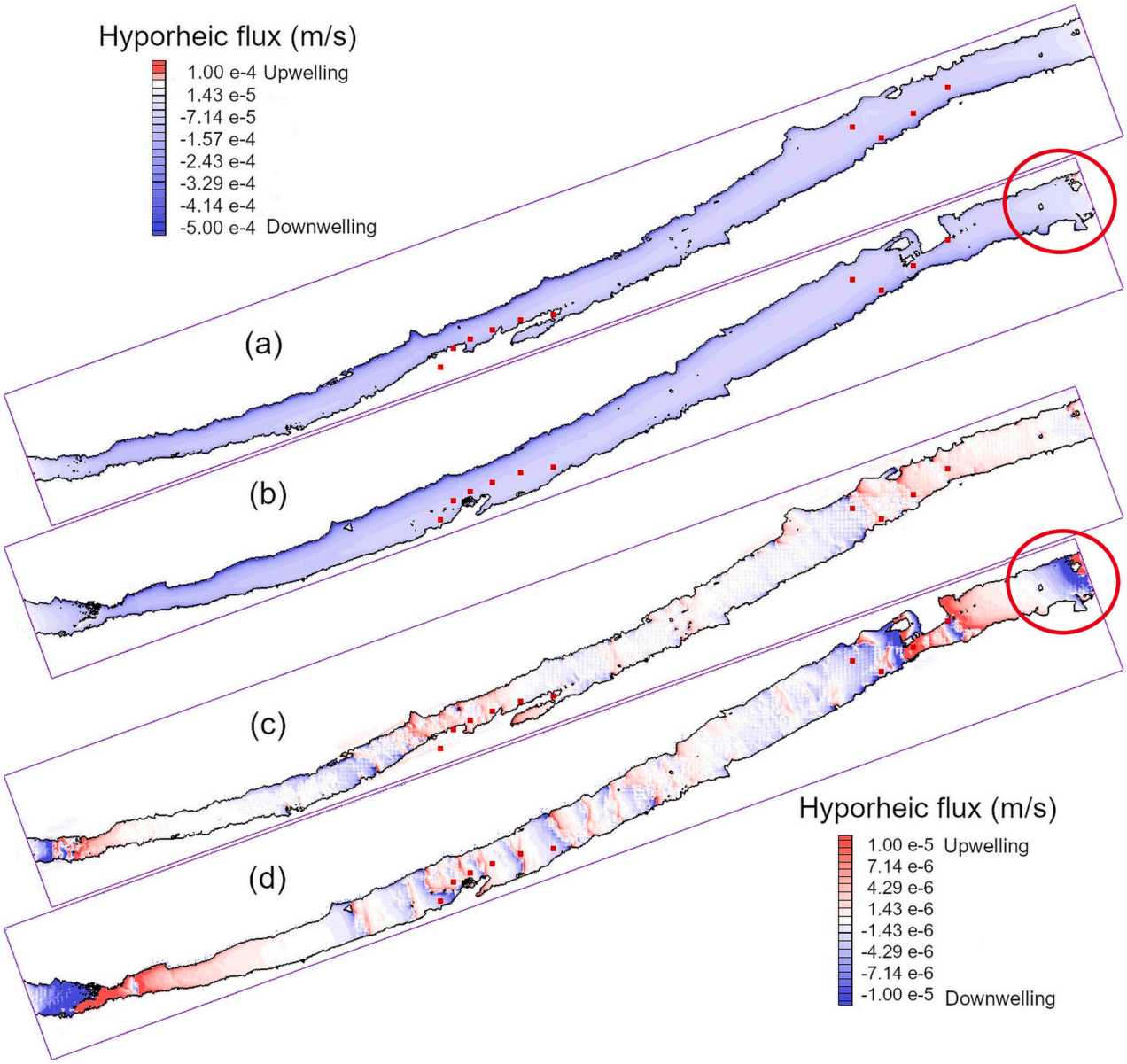

Fig. 9. Hyporheic fluxes for pre (a, c) and post (b, d) flood conditions for losing (a, b) and neutral (c, d) ambient groundwater conditions with probe locations (red squares) at 1.5 m^3/s stream discharge. Positive (red color) fluxes mean upwelling whereas negative (blue color) fluxes mean downwelling. The red circles indicate the location of scour around large boulders, which were in pre-flood conditions mostly imbedded in the streambed. In the post-flood condition is where some hyporheic flows would develop under losing condition.

Table 3
Downwelling and upwelling streambed areas as a function of stream discharge and ambient groundwater conditions.

	Discharge (m^3/s)	Neutral conditions		Losing conditions (21 L/s)	
		Downwelling	Upwelling	Downwelling	Upwelling
		Area (m^2)	Area (m^2)	Area (m^2)	Area (m^2)
Pre-flood	1.9	4323.75	4008.00	8330.75	1.0
	1.5	4348.50	4028.00	8375.50	1.0
	1.1	4277.25	3820.75	8097.50	0.5
	0.86	4177.75	3676.00	7853.00	0.75
	0.31	3701.25	2595.50	6284.50	12.25
Post-flood	1.9	5343.75	4467.50	9778.00	33.25
	1.5	5188.75	4369.25	9525.25	32.75
	1.1	4989.00	4262.75	9222.00	29.75
	0.86	4807.00	4179.75	8957.75	29.00
	0.31	3884.75	3619.25	7482.75	21.25

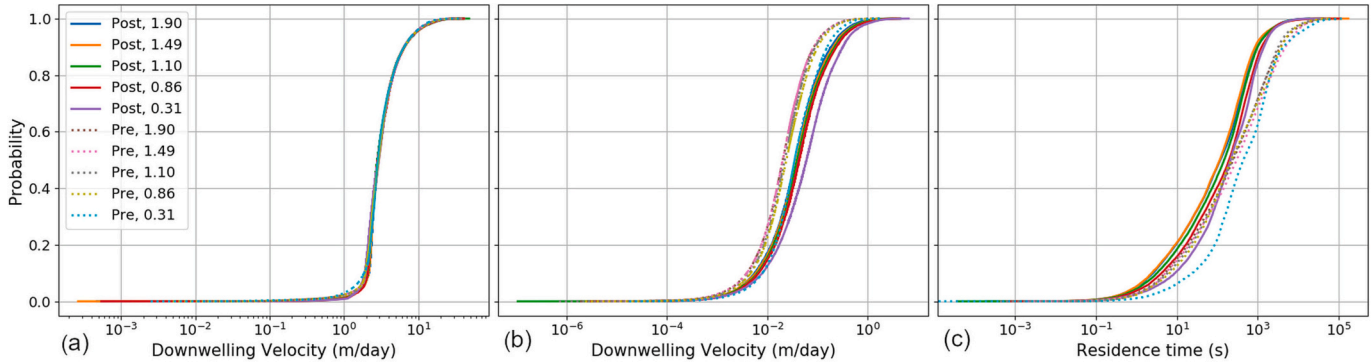

Fig. 10. Near-bed downwelling flux for losing (a) ambient groundwater condition and near bed downwelling velocity (b) and residence time (c) distributions for the neutral for different stream discharges.

flood condition, which would indicate higher streambed permeability. Thus, potentially surface-subsurface water interaction was more limited in the pre-flood conditions.

Increasing hyporheic exchange should increase nutrient removal as more surface water may filter through the streambed, where the microbial community can uptake and transform reactive solutes. The hyporheic exchange can benefit rivers flowing within agricultural fields as they can transform solutes more efficiently. However, this reach is mostly losing such that hyporheic exchange at the bedform scale has limited impact on its water quality through, for instance, nitrification and denitrification processes. However reach scale hyporheic exchange, which is mainly modulated by the interaction between groundwater table and water surface elevation may be important in this stream as it may have longer residence times than bedform induced hyporheic exchange and bring biogeochemical processes to completion, e.g., denitrification (Tonina and Buffington, 2023).

The importance of the boulders and, in general, the alluvial material in the habitat improvement through the creation of hydraulic heterogeneity has been previously analyzed (Branco et al., 2013). More recently, importance of boulders and scour patterns have been recognized in modifying and enhancing hyporheic exchange (Dudunake et al., 2020). However, information is still limited on the synergy of the surface and subsurface hydraulic conditions in creating habitats that mitigate climate change impacts. Such interactions and the potential benefits constitute, therefore, a line of research that can be further developed also with the use of recent development of field sensors (DeWeese et al., 2017) and that can shed new light on habitat improvements concerning aquatic species sensitive to climate change in terms of hydraulics but also stream and pore water temperature.

The increase in morphological complexity and habitat quality is consistent with the idea that pulse events are beneficial disturbances, and the release of high flows from water management structures could have an important effect at the riverscape scale and not just at the reach scale (Suen and Eheart, 2006; Yarnell et al., 2015). Thus, large and frequent flows, $<$ 18 year return period, could be useful and efficient tools for riverine restoration (Chen and Olden, 2017; Groll, 2017; Hayes et al., 2018). For example, some studies considered the intermediate disturbance hypothesis assumption as the basis for defining the fitness function for six eco-hydrological indicators to maintain the livelihood of aquatic ecosystems (Suen and Eheart, 2006). In this context, the consideration of a range of flow events (e.g. high-flow pulses, low flows, etc.) and related ecological processes (e.g. sediment delivery, fish population dynamics, vegetation dynamics, etc.) should be considered to select environmental flow parameters that can be ecologically relevant at a spatial scale larger than the reach-scale, e.g. at the river basin scale (Derepasko et al., 2021; Poff et al., 2017; Yarnell et al., 2015).

Nevertheless, a fundamental question concerns the degree to which the studied flood event contributed to recovering the original natural morphology of the study reach prior to dam construction. We were able to find only one study that documented this issue but only for the first 8 km below the dam (Sanchis-Ibor et al., 2019). Downstream that point, several tributaries and a steep gorge contribute with relevant seasonal flows and sediment supply that make the evaluation difficult. Sanchis-Ibor et al. (2019) studied the channel forms and vegetation adjustment to damming and explained that vegetation, specifically Salicaceae species, played a significant role in controlling flood effectiveness and reducing river mobility in the Serpis River. Regulated flow regime and vegetation encroachment cause the stabilization of channel migration and the transformation from a meandering multi-thread to a fixed single-thread channel. Unregulated flood events that previously caused channel migration were not available post-dam and led to channel stabilization. The vegetation, then dominated by *Salix atrocinerea*, along with other species (e.g., *Salix purpurea*, *Salix eleagnos*, *Arundo donax*, and *Populus nigra*) formed a dense forest gallery along the flowing channel (Sanchis-Ibor et al., 2019).

With different species proportions, this situation resembles the plant diversity in our target river stretch. Although there is no scientific assessment below the gorge (Barranc del Infern), the sediment deficit below the dam can notably change in our case, where the flow and sediment supply below the dam (from hillslopes and tributary streams) can partially compensate for some of the dam's effects. As it was described by previous studies, the local-scale responses to dam regulation in terms of river morphology and sediments dynamics present a relevant variability, reflecting factors such as controls upon sediment yield associated with the availability of sediment from hillslopes or tributary systems (González del Tánago et al., 2015). In addition to the moderate and high erosion rate of the hillslopes in the watershed of the study site, with potential high yields to river channels, the consequences of agriculture development for soil erosion could be relevant to mitigate sediment deficit in our case, as it was demonstrated of great importance in other river basins in Spain and Portugal (Cantón et al., 2011; de Graaff et al., 2010; González del Tánago et al., 2015). Nevertheless, given the dominance of medium-sized substrate in the study site, the fine sediment does not seem to play a fundamental role and there is no sign of aggradation at the local scale. In the present, we hypothesize that the channel is relatively stable in the study site as a consequence of the reduction in the frequency of high flows (Sanchis-Ibor et al., 2019) and the encroachment of vegetation (giant cane) in comparison with the oldest graphical information, as explained below. Both factors have been regarded as fundamental to interpret morphological changes in other Mediterranean rivers, although with much finer sediments (González del Tánago et al., 2015).

The oldest orthophoto available that include our site is dated 1956–57 and was taken just before the dam's closure. It shows a wider single channel with lateral bars and some braided sections nearby, and the riparian vegetation is almost absent on the left bank. In that decade, the watershed below the dam displays dominant natural landscapes (herbs and shrubs in low density) but also a dominant proportion of

agricultural land use around the study site, as well as small weirs diverting flow and bridges crossing the river. In accordance, the forest cover and Mediterranean garrigue seem to display a general positive trend in the watershed. In contrast, previous studies just below the dam indicated that the land-use change in the drainage basin between 1956 and 2009 did not reveal significant changes in terms of effects on sediment yield (Sanchis-Ibor et al., 2019). These observations suggest that further specific studies are required to analyse the biogeomorphic complexity of the watershed in terms of land-use changes (González del Tánago et al., 2015; Graf, 2006), and to give light on the natural original morphology of this river. With the present knowledge, we can assume that the flood event returned the study site to a situation closer to the natural state because the vegetation encroachment was significantly reduced, the channel width increased, there was a significant increase in the bare coarse sediments, and the sediment transport was temporarily activated and new gravel bars developed, resembling the oldest graphical information available. However, further research is needed to assess the degree of recovery and to determine the mid- and long-term effects of this flood event.

The storm's impact on the Serpis River epitomizes the extraordinary power of natural events to reshape and rejuvenate riverine ecosystems. The flood event's consequences extended far beyond the riverbed, affecting the riparian vegetation and the underlying hyporheic zone, a dynamic interface between the stream and the surrounding groundwater. The flood's scouring action uprooted riparian vegetation, particularly dense stands of *Arundo donax*. This disruption fostered the creation of new biogeomorphic features, including gravel bars, side channels, and pools, while simultaneously enhancing the suitability of habitat for some fish species. The flood event's hydromorphological imprint on the Serpis River unveiled the river's inherent resilience and capacity to respond to large and frequent floods. This natural disturbance, akin to a pulse of flooding, served as a catalyst for restoring the river's geomorphological complexity, connectivity, and habitat diversity.

5. Conclusions

Our findings provide support for the Intermediate Disturbance Theory (IDT), indicating that large and frequent floods have positive impacts on stream functioning at various scales. At the local scale, these floods rearrange habitat distribution, enhance habitat diversity, and promote hyporheic exchange. At the reach scale, they contribute to increased streambed complexity and improved lateral and vertical connectivity. We posit that controlled releases of high flow events can serve as an effective strategy to revitalize fluvial forms, riparian habitats, and create opportunities for colonization by pioneer plant species.

Notably the presence of natural features, such as subdued and vegetated side channels, can significantly enhance the success of flood disturbances while reducing the required river discharge for desired renewal, even in the context of regulated flows. This suggests that implementing vegetation management practices, such as small-scale clearing or selective cutting, prior to high flow events can optimize the cost-benefit ratio of these management actions within an environmental flow strategy. This approach may reduce the dependence on high river discharge from reservoirs to achieve the desired ecological and morphological maintenance.

Our results indicate that the utilization of pulse high flows and natural high flows as restoration agents can have significant positive effects throughout entire riverine systems. Contrary to active restoration that typically is limited to few kilometre stream lengths (e.g., Bernhardt et al., 2005), high-flow pulses as they move through the riverine network may reset and enhance riverine and riparian habitats along hundreds of kilometres if not entire riverine lengths and thus are extremely cost-effective. Consequently, we propose that prescribed high flows be considered as highly effective passive restoration techniques for numerous streams and rivers.

Supplementary data to this article can be found online at https://doi.org/10.1016/j.scitotenv.2024.170717.

CRediT authorship contribution statement

Jhoselyn Milagros Aramburú-Paucar: Formal analysis, Investigation, Methodology, Writing – original draft. **Francisco Martínez-Capel:** Conceptualization, Formal analysis, Funding acquisition, Investigation, Methodology, Supervision, Writing – review & editing. **Carlos Antonio Puig-Mengual:** Formal analysis, Methodology, Software. **Rafael Muñoz-Mas:** Formal analysis, Methodology, Software. **Andrea Bertagnoli:** Formal analysis, Methodology, Software. **Daniele Tonina:** Conceptualization, Formal analysis, Investigation, Methodology, Supervision, Writing – review & editing.

Declaration of competing interest

The authors declare that they have no known competing financial interests or personal relationships that could have appeared to influence the work reported in this paper.

Data availability

Data will be made available on request.

Acknowledgement

DT thank the sabbatical program at the University of Idaho and Institut d'Investigació per a la Gestió Integrada de Zones Costaneres (IGIC), Universitat Politècnica de València (UPV), for allowing him to visit Martínez-Capel's research group in the Gandia Campus during the Spring Semester 2020. DT acknowledges support from the Hatch Act (Accession Number IDA01722) through the USDA National Institute of Food and Agriculture. This research was partially funded by the Valencian Government through the Program for the promotion of scientific research, technological development and innovation in the Valencian Community for research groups of excellence, PROMETEO 2021 (ref: PROMETEO/2021/074); and by the European Union's Horizon 2020 - Research and Innovation Framework Programme under the SOS-WATER project (GA no. 101059264).

References

Amoros, C., Roux, A.L., Reygrobellet, J.L., Bravard, J.P., Pautou, G., 1987. A method for applied ecological studies of fluvial hydrosystems. Regul. Rivers Res. Manag. 1, 17–36. https://doi.org/10.1002/rrr.3450010104.

Arcement, G.J., Schneider, V.R., 1984. Guide for Selecting Manning's Roughness Coefficients for Natural Channels and Flood Plains (No. FHWA-TS-84-204). United States. Federal Highway Administration.

Baptist, M.J., Penning, W.E., Duel, H., Smits, A.J.M., Geerling, G.W., Van der Lee, G.E.M., Van Alphen, J.S.L., 2004. Assessment of the effects of cyclic floodplain rejuvenation on flood levels and biodiversity along the Rhine River. River Res. Appl. 20, 285–297. https://doi.org/10.1002/rra.778.

Barbour, M.T., Gerritsen, J., Snyder, B.D., Stribling, J.B., 1999. Rapid Bioassessment Protocols for Use in Streams and Wadeable Rivers: Periphyton, Benthic Macroinvertebrates and Fish, Second Edition, EPA 841-B-99-002. DC, USA, Washington.

Barnes, H.H.J., 1967. Roughness Characteristics of Natural Channels. United States Government Printing Office, Washington, DC.

Benjankar, R., Yager, E., Tonina, D., Merz, N., 2016. REI: riparian ecosystem index to assess the impact of hydrologic regime changes on riparian ecosystems. Ecohydrology 9, 153–166. https://doi.org/10.1002/eco.1621.

Benjankar, R., Tranmer, A.W., Vidergar, D., Tonina, D., 2020. Riparian vegetation model to predict seedling recruitment and restoration alternatives. J. Environ. Manag. 276, 111339 https://doi.org/10.1016/j.jenvman.2020.111339.

Bennetsen, E., Gobeyn, S., Goethals, P.L.M., 2016. Species distribution models grounded in ecological theory for decision support in river management. Ecol. Model. 325, 1–12. https://doi.org/10.1016/j.ecolmodel.2015.12.016.

Bernhardt, E.S., Palmer, M.A., Allan, J.D., Alexander, G., Barnas, K., Brooks, S., Sudduth, E., 2005. Synthesizing US river restoration efforts. Science 308 (5722), 636–637. https://doi.org/10.1126/science.1109769.

Bovee, K.D., 1978. The Incremental Method of assessing habitat potential for cool water species, with management implications. Am. Fish. Soc. Spec. Publ. 11, 340–346.

Bovee, K.D., 1982. A guide to stream habitat analysis using the instream flow incremental methodology. In: Western Energy and Land Use Team. Office of Biological Services, Fish and Wildlife Service, US Department of the Interior.
Bovee, K.D., Lamb, B.L., Bartholow, J.M., Stalnaker, C.B., Taylor, J., Henriksen, J., 1998. Stream Habitat Analysis Using the Instream Flow Incremental Methodology. U.S, Geological Survey, Biological Resources Division Information and Technology.
Branco, P., Boavida, I., Santos, J.M., Pinheiro, A., Ferreira, M.T., 2013. Boulders as building blocks: improving habitat and river connectivity for stream fish. Ecohydrology 6 (4), 627–634. https://doi.org/10.1002/eco.1290.
Brandt, S.A., 2000. Classification of geomorphological effects downstream of dams. CATENA 40, 375–401. https://doi.org/10.1016/S0341-8162(00)00093-X.
Brasington, J., Langham, J., Rumsby, B., 2003. Methodological sensitivity of morphometric estimates of coarse fluvial sediment transport. Geomorphology 53 (3–4), 299–316. https://doi.org/10.1016/S0169-555X(02)00320-3.
Bray, E.N., Dunne, T., 2017. Observations of bedload transport in a gravel bed river during high flow using fiber-optic DTS methods. Earth Surf. Process. Landf. 42 (13), 2184–2198. https://doi.org/10.1002/esp.4164.
Bunn, S.E., Arthington, A.H., 2002. Basic principles and ecological consequences of altered flow regimes for aquatic biodiversity. Environ. Manag. 30, 492–507. https://doi.org/10.1007/s00267-002-2737-0.
Calle, M., Alho, P., Benito, G., 2018. Monitoring ephemeral river changes during floods with SfM photogrammetry. J. Iber. Geol. 44 (3), 355–373. https://doi.org/10.1007/s41513-018-0078-y.
Calvani, G., Francalanci, S., Solari, L., 2019. A physical model for the uprooting of flexible vegetation on river bars. Case Rep. Med. 124, 1018–1034. https://doi.org/10.1029/2018JF004747.
Cantón, Y., Solé-Benet, A., de Vente, J., Boix-Fayos, C., Calvo-Cases, A., Asensio, C., Puigdefábregas, J., 2011. A review of runoff generation and soil erosion across scales in semiarid south-eastern Spain. J. Arid Environ. 75, 1254–1261. https://doi.org/10.1016/j.jaridenv.2011.03.004.
Carnie, R., Tonina, D., McKean, J.A., Isaak, D.J., 2015. Habitat connectivity as a metric for aquatic microhabitat quality: application to Chinook salmon spawning habitat. Ecohydrology 9, 982–994. https://doi.org/10.1002/eco.1696.
Chen, W., Olden, J.D., 2017. Designing flows to resolve human and environmental water needs in a dam-regulated river. Nat. Commun. 8, 2158. https://doi.org/10.1038/s41467-017-02226-4.
Church, M., 1995. Geomorphic response to river flow regulation: case studies and time-scales. Regul. Rivers Res. Manag. 11, 3–22. https://doi.org/10.1002/rrr.3450110103.
Conesa-García, C., Puig-Mengual, C., Riquelme, A., Tomás, R., Martínez-Capel, F., García-Lorenzo, R., Pastor, J.L., Pérez-Cutillas, P., Cano Gonzalez, M., 2020. Combining SfM photogrammetry and terrestrial laser scanning to assess event-scale sediment budgets along a gravel-bed ephemeral stream. Remote Sens. 12, 3624. https://doi.org/10.3390/rs12213624.
Conesa-García, C., Puig-Mengual, C., Riquelme, A., Tomás, R., Martínez-Capel, F., García-Lorenzo, R., Pastor, J.L., Pérez-Cutillas, P., Martínez-Salvador, A., Cano-Gonzalez, M., 2022. Changes in stream power and morphological adjustments at the event-scale and high spatial resolution along an ephemeral gravel-bed channel. Geomorphology 398, 108053. https://doi.org/10.1016/j.geomorph.2021.108053.
Confederación Hidrográfica del Júcar, 2008. Proyecto de restauración del río Serpis en los TT. MM. de Lorcha (provincia de Alicante) y Villalonga (provincia de Valencia).
Confederación Hidrográfica del Júcar, 2019. Demarcación Hidrográfica del Júcar. Revisión y actualización de los mapas de peligrosidad y riesgo de inundación (2º Ciclo). Memoria.
Cortés, F.M., Molina, B., Magdaleno, F., 2019. Crecidas controladas en el río Manzanares para la mejora del régimen de caudales ecológicos. In: III Congreso Ibéric de Restauración Fluvial, RESTAURARIOS. RESTAURARIOS. Iberian Centre for River Restoration, Zaragoza, Spain.
Curto, M., Morgado-Santos, M., Alexandre, C.M., Alves, M.J., Gante, H.F., Gkenas, C., Medeiros, J.P., Pinheiro, P.J., Almeida, P.R., Magalhães, M.F., Ribeiro, F., 2022. Widespread hybridization between invasive bleak (Alburnus alburnus) and Iberian chub (Squalius spp.): a neglected conservation threat. Fishes 7, 247. https://doi.org/10.3390/fishes7050247.
Dean, D.J., Schmidt, J.C., 2013. The geomorphic effectiveness of a large flood on the Rio Grande in the Big Bend region: insights on geomorphic controls and post-flood geomorphic response. Geomorphology 201, 183–198. https://doi.org/10.1016/j.geomorph.2013.06.020.
Derepasko, D., Guillaume, J.H.A., Horne, A.C., Volk, M., 2021. Considering scale within optimization procedures for water management decisions: balancing environmental flows and human needs. Environ. Model Softw. 139, 104991 https://doi.org/10.1016/j.envsoft.2021.104991.
DeWeese, T., Tonina, D., Luce, C., 2017. Monitoring streambed scour/deposition under nonideal temperature signal and flood conditions. Water Resour. Res. 53 https://doi.org/10.1002/2017WR020632.
Dudunake, T., Tonina, D., Reeder, W.J., Monsalve, A., 2020. Local and reach-scale hyporheic flow response from boulder-induced geomorphic changes. Water Resour. Res. 56 (10), e2020WR027719 https://doi.org/10.1029/2020WR027719.
Duffin, J., Yager, E.M., Buffington, J.M., Benjankar, R., Borden, C., Tonina, D., 2023. Impact of flow regulation on stream morphology and habitat quality distribution. Sci. Total Environ. 878 https://doi.org/10.1016/j.scitotenv.2023.163016.
Džubáková, K., Molnar, P., Schindler, K., Trizna, M., 2015. Monitoring of riparian vegetation response to flood disturbances using terrestrial photography. Hydrol. Earth Syst. Sci. 19, 195–208. https://doi.org/10.5194/hess-19-195-2015.
Escobar-Arias, M.I., Pasternack, G.B., 2010. A hydrogeomorphic dynamics approach to assess in-stream ecological functionality using the functional flows model, part 1-model characterstics. River Res. Appl. 26, 1103–1128.
García, A., Jorde, K., Habit, E., Caamaño, D., Parra, O., 2011. Downstream environmental effects of dam operations: changes in habitat quality for native fish species. River Res. Appl. 27, 312–327.
García-Ortuño, T., Ferrández-García, M.T., Andreu-Rodríguez, J., Ferrández-Villena, M., Ferrandez-Garcia, C.E., 2014. Study of the mechanical properties of giant reed as a green building material. In: Second Intl. Conf. on Advances in Civil, Structural and Environmental Engineering-ACSEE 2014. Institute of Research Engineers and Doctors, USA, pp. 165–167. https://doi.org/10.15224/978-1-63248-030-9-34.
Gariglio, F.P., Tonina, D., Luce, C.H., 2013. Spatio-temporal variability of hyporheic exchange through a pool-riffle-pool sequence. Water Resour. Res. 49, 7185–7204. https://doi.org/10.1002/wrcr.20419.
Garófano-Goméz, V., Martínez-Capel, F., Peredo-Parado, M., Olaya Marín, E.J., Muñoz Mas, R., Soares Costa, R.M., Pinar-Arenas, J.L., 2011. Assessing hydromorphological and floristic patterns along a regulated Mediterranean river: the Serpis River (Spain). Limnetica 30, 307–328. https://doi.org/10.23818/limn.30.23.
Garófano-Gómez, V., Jean-François Corenblit, D., Steiger, J., Moulia, B., Ploquin, S., Chaleil, P., Forestier, O., Evette, A., González, E., Hortobágyi, B., Corenblit, D., Lambs, L., 2016. Response of black poplar (Populus nigra L.) to hydrogeomorphological constraints: a semi-controlled ex situ experiment. In: 5th International EcoSummit 2016. Ecological Sustainability: Engineering Change.
Gobeyn, S., Volk, M., Dominguez-Granda, L., Goethals, P.L.M., 2017. Input variable selection with a simple genetic algorithm for conceptual species distribution models: a case study of river pollution in Ecuador. Environ. Model Softw. 92, 269–316. https://doi.org/10.1016/j.envsoft.2017.02.012.
González del Tánago, M., Bejarano, M.D.D., García de Jalón, D., Schmidt, J.C.C., 2015. Biogeomorphic responses to flow regulation and fine sediment supply in Mediterranean streams (the Guadalete River, southern Spain). J. Hydrol. 528, 751–762. https://doi.org/10.1016/j.jhydrol.2015.06.065.
Gordon, R.P., Lautz, L.K., Daniluk, T.L., 2013. Spatial patterns of hyporheic exchange and biogeochemical cycling around cross-vane restoration structures: implications for stream restoration design. Water Resour. Res. 49, 2040–2055. https://doi.org/10.1002/wrcr.20185.
Gostner, W., Alp, M., Schleiss, A.J., Robinson, C.T., 2013. The hydro-morphological index of diversity: a tool for describing habitat heterogeneity in river engineering projects. Hydrobiologia 712, 43–60. https://doi.org/10.1007/s10750-012-1288-5.
de Graaff, J., Duarte, F., Fleskens, L., de Figueiredo, T., 2010. The future of olive groves on sloping land and ex-ante assessment of cross compliance for erosion control. Land Use Policy 27, 33–41. https://doi.org/10.1016/j.landusepol.2008.02.006.
Graf, W.L., 2006. Downstream hydrologic and geomorphic effects of large dams on American rivers. Geomorphology 79, 336–360. https://doi.org/10.1016/j.geomorph.2006.06.022.
Grant, G., Schmidt, J., Lewis, S., 2003. A geological framework for interpreting downstream effects of dams on rivers. A Peculiar River. Am. Geophys. Union, Water Sci. Appl. 203–219.
Groll, M., 2017. The passive river restoration approach as an efficient tool to improve the hydromorphological diversity of rivers – case study from two river restoration projects in the German lower mountain range. Geomorphology 293, 69–83. https://doi.org/10.1016/j.geomorph.2017.05.004.
Gurnell, A.M., Bertoldi, W., 2020. Extending the conceptual model of river island development to incorporate different tree species and environmental conditions. River Res. Appl. 36, 1730–1747. https://doi.org/10.1002/rra.3691.
Gurnell, A., Tockner, K., Edwards, P., Petts, G., 2005. Effects of deposited wood on biocomplexity of river corridors. Front. Ecol. Environ. 3, 377–382. https://doi.org/10.1890/1540-9295(2005)003[0377:EODWOB]2.0.CO;2.
Hajdukiewicz, H., Wyżga, B., Mikuś, P., Zawiejska, J., Radecki-Pawlik, A., 2016. Impact of a large flood on mountain river habitats, channel morphology, and valley infrastructure. Geomorphology 272, 55–67. https://doi.org/10.1016/j.geomorph.2015.09.003.
Hajdukiewicz, H., Wyżga, B., Amirowicz, A., Oglęcki, P., Radecki-Pawlik, A., Zawiejska, J., Mikuś, P., 2018. Ecological state of a mountain river before and after a large flood: implications for river status assessment. Sci. Total Environ. 610–611, 244–257. https://doi.org/10.1016/j.scitotenv.2017.07.162.
Harezlak, V., Augustijn, D.C.M., Geerling, G.W., van Geest, G.J., Leuven, R.S.E.W., 2020a. Linking plant strategies to environmental processes in floodplains of lowland rivers. J. Hydrol. Res. 30, 45–62. https://doi.org/10.1016/j.jher.2020.01.002.
Harezlak, V., Geerling, G.W., Rogers, C.K., Penning, W.E., Augustijn, D.C.M., Hulscher, S.J.M.H., 2020b. Revealing 35 years of landcover dynamics in floodplains of trained lowland rivers using satellite data. River Res. Appl. 36, 1213–1221. https://doi.org/10.1002/rra.3633.
Hayes, D.S., Brändle, J.M., Seliger, C., Zeiringer, B., Ferreira, T., Schmutz, S., 2018. Advancing towards functional environmental flows for temperate floodplain rivers. Sci. Total Environ. 633, 1089–1104. https://doi.org/10.1016/j.scitotenv.2018.03.221.
Jorde, K., Schneider, M., Peter, A., Zoellner, F., 2001. Fuzzy based models for the evaluation of fish habitat quality and instream flow assessment. In: Proc. 3rd Int. Symp. Environ. Hydraul. 5–8 December, Tempe, AZ, pp. 1–6.
Kammel, L.E., Pasternack, G.B., Massa, D.A., Bratovich, P.M., 2016. Near-census ecohydraulics bioverification of *Oncorhynchus mykiss* spawning microhabitat preferences. J. Ecohydraulics 1, 62–78. https://doi.org/10.1080/24705357.2016.1237264.
Lama, G.F.C., Errico, A., Pasquino, V., Mirzaei, S., Preti, F., Chirico, G.B., 2022. Velocity uncertainty quantification based on Riparian vegetation indices in open channels colonized by Phragmites australis. J. Ecohydraulics 7, 71–76. https://doi.org/10.1080/24705357.2021.1938255.

Ligon, F.K., Dietrich, W.E., Trush, W.J., 1995. Downstream ecological effects of dams - a geomorphic perspective. Bioscience 45, 183–192. https://doi.org/10.2307/1312557.

Luce, C.H., Tonina, D., Gariglio, F., Applebee, R., 2013. Solutions for the diurnally forced advection-diffusion equation to estimate bulk fluid velocity and diffusivity in streambeds from temperature time series. Water Resour. Res. 49, 488–506. https://doi.org/10.1029/2012WR012380.

Mezger, G., De Stefano, L., González del Tánago, M., 2019. Assessing the establishment and implementation of environmental flows in Spain. Environ. Manag. 64, 721–735. https://doi.org/10.1007/s00267-019-01222-2.

Mikuś, P., Wyzga, B., Kaczka, R.J., Walusiak, E., Zawiejska, J., 2013. Islands in a European mountain river: linkages with large wood deposition, flood flows and plant diversity. Geomorphology 202, 115–127. https://doi.org/10.1016/j.geomorph.2012.09.016.

Montgomery, D.R., Buffington, J.M., 1998. Channel processes, classification, and response. In: Naiman, R.J., Bilby, R. (Eds.), River Ecology and Management. Springer-Verlag, New York, pp. 13–42.

Mouton, A.M., Schneider, M., Peter, A., Holzer, G., Müller, R., Goethals, P.L.M., De Pauw, N., 2008. Optimisation of a fuzzy physical habitat model for spawning European grayling (*Thymallus thymallus* L.) in the Aare river (Thun, Switzerland). Ecol. Model. 215, 122–132. https://doi.org/10.1016/j.ecolmodel.2008.02.028.

Mouton, A.M., Alcaraz-Hernández, J.D., De Baets, B., Goethals, P.L.M., Martínez-Capel, F., 2011. Data-driven fuzzy habitat suitability models for brown trout in Spanish Mediterranean rivers. Environ. Model Softw. 26, 615–622. https://doi.org/10.1016/j.envsoft.2010.12.001.

Muñoz-Mas, R., Martínez-Capel, F., Schneider, M., Mouton, A.M., 2012. Assessment of brown trout habitat suitability in the Jucar River Basin (Spain): comparison of data-driven approaches with fuzzy-logic models and univariate suitability curves. Sci. Total Environ. 440, 123–131. https://doi.org/10.1016/j.scitotenv.2012.07.074.

Muñoz-Mas, R., Papadaki, C., Martínez-Capel, F., Zogaris, S., Ntoanidis, L., Dimitriou, E., 2016. Generalized additive and fuzzy models in environmental flow assessment: a comparison employing the West Balkan trout (*Salmo farioides*; Karaman, 1938). Ecol. Eng. 91, 365–377. https://doi.org/10.1016/j.ecoleng.2016.03.009.

Muñoz-Mas, R., Fukuda, S., Pórtoles, J., Martínez-Capel, F., 2018a. Revisiting probabilistic neural networks: a comparative study with support vector machines and the microhabitat suitability for the Eastern Iberian chub (Squalius valentinus). Ecol. Inform. 43, 24–37. https://doi.org/10.1016/J.ECOINF.2017.10.008.

Muñoz-Mas, R., Marcos-Garcia, P., Lopez-Nicolas, A., Martínez-García, F.J., Pulido-Velazquez, M., Martínez-Capel, F., 2018b. Combining literature-based and data-driven fuzzy models to predict brown trout (*Salmo trutta* L.) spawning habitat degradation induced by climate change. Ecol. Model. 386, 98–114. https://doi.org/10.1016/j.ecolmodel.2018.08.012.

Muñoz-Mas, R., Gil-Martínez, E., Oliva-Paterna, F.J., Belda, E.J., Martínez-Capel, F., 2019. Tree-based ensembles unveil the microhabitat suitability for the invasive bleak (*Alburnus alburnus* L.) and pumpkinseed (*Lepomis gibbosus* L.): introducing XGBoost to eco-informatics. Ecol. Inform. 53 https://doi.org/10.1016/j.ecoinf.2019.100974.

Nilsson, C., Reidy, C.A., Dynesius, M., Revenga, C., 2005. Fragmentation and flow regulation of the world's large river systems. Science (80-.) 308, 405–408. https://doi.org/10.1126/science.1107887.

Noack, M., Schneider, M., Wieprecht, S., 2013. The habitat modelling system CASiMiR: a multivariate fuzzy approach and its applications. In: Maddock, I., Wood, P.J., Harby, A., Kemp, P. (Eds.), Ecohydraulics: An Integrated Approach. Wiley-Blackwell, New Delhi, India, pp. 75–91.

Perea, S., Doadrio, I., 2015. Phylogeography, historical demography and habitat suitability modelling of freshwater fishes inhabiting seasonally fluctuating mediterranean river systems: a case study using the iberian cyprinid Squalius valentinus. Mol. Ecol. 24 https://doi.org/10.1111/mec.13274.

Petts, G.E., Gurnell, A.M., 2022. Hydrogeomorphic effects of reservoirs, dams, and diversions, in: Treatise on Geomorphology. Elsevier, pp. 144–166. doi:https://doi.org/10.1016/B978-0-12-818234-5.00034-1.

Poff, L.N., Zimmermann, J.K.H., 2010. Ecological responses to altered flow regimes: a literature review to 987 inform the science and management of environmental flows. Freshw. Biol. 55, 194–205.

Poff, L.N., Allan, J.D., Bain, M.B., Karr, J.R., Prestegaard, K.L., Richter, B.D., Sparks, R.E., Stromberg, J.C., 1997. The natural flow regime: a paradigm for river conservation and restoration. Bioscience 47, 769–784.

Poff, N.L., Tharme, R.E., Arthington, A.H., 2017. Evolution of environmental flows assessment science, principles, and methodologies. In: Water for the Environment. Elsevier, pp. 203–236. https://doi.org/10.1016/B978-0-12-803907-6.00011-5.

Puig-Mengual, C.A., Woodget, A.S., Muñoz-Mas, R., Martínez-Capel, F., 2021. Spatial validation of submerged fluvial topographic models by mesohabitat units. Int. J. Remote Sens. 42, 2391–2416. https://doi.org/10.1080/01431161.2020.1862433.

Revelli, R., Boano, F., Camporeale, C., Ridolfi, L., 2008. Intra-meander hyporheic flow in alluvial rivers. Water Resour. Res. 44, W12428.

Richter, B.D., Mathews, R., Harrison, D.L., Wigington, R., 2003. Ecologically sustainable water management: managing river flows for ecological integrity. Ecol. Appl. 13, 206–224. https://doi.org/10.1890/1051-0761(2003)013.

Sanchis-Ibor, C., Segura-Beltrán, F., Navarro-Gómez, A., 2019. Channel forms and vegetation adjustment to damming in a Mediterranean gravel-bed river (Serpis River, Spain). River Res. Appl. 35, 37–47. https://doi.org/10.1002/rra.3381.

Schmidt, J.C., Wilcock, P.R., 2008. Metrics for assessing the downstream effects of dams. Water Resour. Res. 44 https://doi.org/10.1029/2006WR005092.

Seifert, E., Seifert, S., Vogt, H., Drew, D., van Aardt, J., Kunneke, A., Seifert, T., 2019. Influence of drone altitude, image overlap, and optical sensor resolution on multi-view reconstruction of forest images. Remote Sens. 11, 1252. https://doi.org/10.3390/rs11101252.

Suen, J.-P., Eheart, J.W., 2006. Reservoir management to balance ecosystem and human needs: incorporating the paradigm of the ecological flow regime. Water Resour. Res. 42 https://doi.org/10.1029/2005WR004314.

Takagi, T., Sugeno, M., 1985. Fuzzy identification of systems and its applications to modeling and control. IEEE Trans. Syst. Man Cybern. 15, 116–132. https://doi.org/10.1109/TSMC.1985.6313399.

Talbot, C.J., Bennett, E.M., Cassell, K., Hanes, D.M., Minor, E.C., Paerl, H., Raymond, P. A., Vargas, R., Vidon, P.G., Wollheim, W., Xenopoulos, M.A., 2018. The impact of flooding on aquatic ecosystem services. Biogeochemistry 141, 439–461. https://doi.org/10.1007/s10533-018-0449-7.

Tonina, D., Buffington, J.M., 2009. Hyporheic exchange in mountain rivers I: mechanics and environmental effects. Geogr. Compass 3, 1063–1086. https://doi.org/10.1111/j.1749-8198.2009.00226.x.

Tonina, D., Buffington, J.M., 2023. Physical and biogeochemical processes of hyporheic exchange in alluvial rivers. Groundw. Ecol. Evol. 61–87. https://doi.org/10.1016/B978-0-12-819119-4.15001-2.

Tonina, D., Luce, C.H., Gariglio, F., 2014. Quantifying streambed deposition and scour from stream and hyporheic water temperature time series. Water Resour. Res. 50, 287–292. https://doi.org/10.1002/2013WR014567.

Tonina, D., McKean, J.A., Benjankar, R.M., Yager, E., Carmichael, R.A., Chen, Q., Carpenter, A., Kelsey, L.G., Edmondson, M.R., 2020. Evaluating the performance of topobathymetric LiDAR to support multi-dimensional flow modelling in a gravel-bed mountain stream. Earth Surf. Process. Landf. 45, 2850–2868. https://doi.org/10.1002/esp.4934.

Townsend, C.R., Scarsbrook, M.R., Dolédec, S., 1997. The intermediate disturbance hypothesis, refugia, and biodiversity in streams. Limnol. Oceanogr. 42, 938–949. https://doi.org/10.4319/lo.1997.42.5.0938.

Vannote, R.L., Minshall, W.G., Cummins, K.W., Sedell, J.R., Cushing, C.E., 1980. The river continuum concept. Can. J. Fish. Aquat. Sci. 37, 130–137.

Ward, J.V., 1989. The four-dimensional nature of lotic ecosystems. J. North Am. Benthol. Soc. 8, 2–8. https://doi.org/10.2307/1467397.

Ward, J.V., Stanford, J.A., 1983. The intermediate-disturbance hypothesis: an explanation for biotic diversity patterns in lotic ecosystem. In: Bartell, S., Fontaine, T. (Eds.), Dynamics of Lotix Ecosystems. Ann Arbor Science, Ann Arbor, Michigan.

Ward, J.V., Stanford, J.A., 1995. The serial discontinuity concept: extending the model to floodplain rivers. Regul. Rivers Res. Manag. 10, 159–168.

Wheaton, J.M., Brasington, J., Darby, S.E., Merz, J., Pasternack, G.B., Sear, D., Vericat, D., 2010a. Linking geomorphic changes to salmonid habitat at a scale relevant to fish. River Res. Appl. 26, 469–486. https://doi.org/10.1002/rra.1305.

Wheaton, J.M., Brasington, J., Darby, S.E., Sear, D.A., 2010b. Accounting for uncertainty in DEMs from repeat topographic surveys: improved sediment budgets. Earth Surf. Process. Landf. 35, 136–156.

Williams, G.P., Wolman, M.G., 1984. Downstream effects of dams on alluvial rivers. In: U.S. Geol. Surv. Prof. Pap..

Wohl, E., Kramer, N., Ruiz-Villanueva, V., Scott, D.N., Comiti, F., Gurnell, A.M., Piegay, H., Lininger, K.B., Jaeger, K.L., Walters, D.M., Fausch, K.D., 2019. The natural wood regime in rivers. Bioscience 69, 259–273. https://doi.org/10.1093/biosci/biz013.

Yarnell, S.M., Petts, G.E., Schmidt, J.C., Whipple, A.A., Beller, E.E., Dahm, C.N., Goodwin, P., Viers, J.H., 2015. Functional flows in modified riverscapes: hydrographs, habitats and opportunities. Bioscience. https://doi.org/10.1093/biosci/biv102.

Yavno, S., Gobin, J., Wilson, C.C., Vila-Gispert, A., Copp, G.H., Fox, M.G., 2020. New and Old World phylogeography of pumpkinseed *Lepomis gibbosus* (Linnaeus, 1758): the North American origin of introduced populations in Europe. Hydrobiologia 847, 345–364. https://doi.org/10.1007/s10750-019-04095-y.

Zadeh, L.A., 1965. Fuzzy sets. Inf. Control. 8, 338–353. https://doi.org/10.1016/S0019-9958(65)90241-X.